ROBUST CLOCK SYNCHRONIZATION IN WIRELESS SENSOR NETWORKS

A Thesis

by

SAWIN SAIBUA

Submitted to the Office of Graduate Studies of
Texas A&M University
in partial fulfillment of the requirements for the degree of

MASTER OF SCIENCE

August 2010

Major Subject: Electrical Engineering

Robust Clock Synchronization in Wireless Sensor Networks

ROBUST CLOCK SYNCHRONIZATION IN WIRELESS SENSOR NETWORKS

A Thesis

by

SAWIN SAIBUA

Submitted to the Office of Graduate Studies of
Texas A&M University
in partial fulfillment of the requirements for the degree of

MASTER OF SCIENCE

Approved by:

Chair of Committee,	Erchin Serpedin
Committee Members,	Deepa Kundur
	Aydin I. Karsilayan
	Radu Stoleru
Head of Department,	Costas Georghiades

August 2010

Major Subject: Electrical Engineering

ABSTRACT

Robust Clock Synchronization in Wireless Sensor Networks. (August 2010)

Sawin Saibua, B.Eng., Chulalongkorn University

Chair of Advisory Committee: Dr. Erchin Serpedin

Clock synchronization between any two nodes in a Wireless Sensor Network (WSNs) is generally accomplished through exchanging messages and adjusting clock offset and skew parameters of each node's clock. To cope with unknown network message delays, the clock offset and skew estimation schemes have to be reliable and robust in order to attain long-term synchronization and save energy.

A joint clock offset and skew estimation scheme is studied and developed based on the Gaussian Mixture Kalman Particle Filter (GMKPF). The proposed estimation scheme is shown to be a more flexible alternative than the Gaussian Maximum Likelihood Estimator (GMLE) and the Exponential Maximum Likelihood Estimator (EMLE), and to be a robust estimation scheme in the presence of non-Gaussian/non-exponential random delays. This study also includes a sub optimal method called Maximum Likelihood-like Estimator (MLLE) for Gaussian and exponential delays.

The computer simulations illustrate that the scheme based on GMKPF yields better results in terms of Mean Square Error (MSE) relative to GMLE, EMLE, GMLLE, and EMLLE, when the network delays are modeled as non-Gaussian/non-exponential distributions or as a mixture of several distributions.

ACKNOWLEDGEMENTS

I would like to thank my committee chair, Dr. Serpedin, and my committee members, Dr. Kundur, Dr. Karsilayan, and Dr. Stoleru, for their guidance and support throughout the course of this research.

I also would like to extend my gratitude to Dr. Jangsub Kim and Jaehan Lee who sacrificed their time to help me on my research. Thanks also go to my friends and colleagues and the department faculty and staff for making my time at Texas A&M University a great experience.

Finally, thanks to my parents for their great encouragement and love.

TABLE OF CONTENTS

CHAPTER Page

LIST OF FIGURES

FIGURE Page

FIGURE Page

CHAPTER I

INTRODUCTION

1.1 Wireless Sensor Networks and Their Applications

Advancement in Micro-Electro-Mechanical systems (MEMS), wireless communications and digital electronics has allowed the development of small, low-cost, energy efficient, and multi-functional wireless sensing devices. Wireless sensors are featured in general with environmental sensing and data processing capabilities, and with means to freely communicate over short distance. This enables the sensor nodes to efficiently collaborate for collecting and processing information and to effectively operate over a large region. A system composed of a large number of sensor nodes is called a Wireless Sensor Network (WSN) [1], [2].

Given the promising features of WSNs, the number of applications involving WSNs has grown rapidly, and as a result, WSNs have found a wide range of practical applications in health, military, environment, trading, security, etc. For example, in a hospital, sensor networks can remotely monitor the patient's physiological data and allow doctors to identify pre-determined symptoms in earlier stages. WSNs can relay the origin of wild fire by strategically, randomly, and densely deploying the sensor nodes in the forest. They can be embedded into home appliances such as TVs, refrigerators, and micro-waves and can be controlled locally and remotely by users. As a consequence, in the near future, WSNs could be integrated into many aspects of a person's daily life [2].

This thesis follows the style of *IEEE Transactions on Automatic Control*.

There are many factors which influence the design of WSNs such as nodes' fault tolerance, scalability, production costs, operation environments, network topology, hardware constraints, transmission media, and power consumption [2]. Especially, the sensor nodes' power is limited because the scale of deployment makes them mostly inaccessible and their batteries are restricted in terms of power levels. In addition, data communication is the most vital operation in WSNs and requires huge portion of energy consumption which in general is greater than the energy required by the local data processing at each individual sensor node. Therefore, the most crucial factor in designing WSNs is to ensure the energy efficiency.

1.2 Importance of Robust Clock Synchronization

In any distributed systems, clock synchronization is a critical piece of infrastructure because it is a procedure for providing a common knowledge of time across the entire system which allows collaboration among the nodes in the system. WSN is an example of such a distributed system that needs clock synchronization in order to perform a number of fundamental operations such as data fusion, power management, transmission scheduling, tracking, etc. [1].

Every individual sensor node in a network has its own clock function defined by its clock offset and skew parameters. Clock synchronization between any two nodes is generally accomplished by message exchanges. Due to the presence of non-deterministic and possibly unbounded message delays, messages can be delayed arbitrarily while transferring messages between any two nodes. This makes the clock synchronization a

difficult and complex problem. The most commonly proposed non-deterministic network delay distributions are the Gaussian, Exponential, Gamma, and Weibull probability density functions (pdfs) [3], [4], [5], [6]. The maximum likelihood estimators (MLEs) of clock offset and clock skew have been proposed for the Gaussian delay model and Exponential Delay model in [3], [7], respectively. However, paper [8] shows that MLE for the Gaussian delay model (GMLE) and the MLE for the Exponential delay model (EMLE) are quite sensitive to the network delay distribution. Consequently, any uncertainty in the knowledge of network delay distribution increases the number of message errors and the number of message retransmissions, which cause WSNs to waste more power to achieve synchronization. Therefore, robust clock synchronization techniques for WSNs are required to withstand the unknown or possibly time-varying distributions of the network delays in the uplink and downlink of message exchanges. In any distributed system, clock synchronization is a critical piece of infrastructure because it is a procedure for providing a common knowledge of time across the entire system which allows collaboration among nodes in the system. WSNs are one of such systems that need clock synchronization in order to perform a number of fundamental operations such as data fusion, power management, transmission scheduling, tracking, etc [1].

Reference [4] proposes a robust clock offset estimation method in the presence of non-Gaussian random delays, referred to as the Gaussian Mixture Kalman Particle Filter (GMKPF). The Mean-Square Error (MSE) performance of GMKPF is superior than the MSE performance of GMLE and EMLE in general network delay distributions and in the presence of a small number of message exchanges. A reduced number of message

exchanges helps WSNs consume less energy which is one of the most important points in designing WSNs. This thesis proposes to study a joint clock offset and skew estimation method based on GMKPF. The MSE performance of GMKPF, GMLE, and EMLE is simulated under Gaussian, Exponential, Gamma, Weibull delay distributions, and a mixing of two delay distributions. The computer simulation results show that the proposed scheme has superior performance relative to GMLE and EMLE in most network delay distributions. Therefore, GMKPF represents a very reliable scheme for joint clock offset and skew estimation. This will help guarantee long-term reliability of clock synchronization and reduce network-wide energy consumption, which is one of the key strategies for the successful deployment of long-lived WSNs.

1.3 Literature Review

A few protocols have been proposed for clock synchronization of WSNs. This research analyzes the clock sync protocols relying on two-way message exchanges between two nodes. The adopted scenario is similar to the Timing synch Protocol for Sensor Networks (TPSN) [9]. TPSN acts as a conventional sender-receiver protocol which assumes two operational stages: the level discovery phase and the synchronization phase. The global synchronization of the network is achieved by the two-way message exchanging mechanism through adjusting only its clock offset.

By applying a probabilistic approach to deal with the clock synchronization problem in WSNs, Abdel-Ghaffar [3] classified the link delay as deterministic and non-deterministic components. Abdel-Ghaffar also reviews five different clock offset

estimation algorithms which include the median round delay, the minimum round delay, the median phase, and the average phase under symmetric exponential link delay. Later, Jeske [10] mathematically proved that MLE of clock offset exists when the fixed delay components in each direction are equal and the variable delay is exponentially distribution with an unknown mean. This result was also consistent with the previously proposed estimators. In a work of Noh et al. [8], MLE for the symmetric Gaussian delay model was derived and the Joint Maximum Likelihood Estimator (JMLE) of clock offset and clock skew for the symmetric Gaussian model delay was also derived. In addition, Noh et al. [8] also proposed a less computationally complex method for clock offset and skew estimation under Gaussian and exponential delays, called the Maximum Likelihood-Like Estimator (MLLE). Furthermore, JMLE of clock offset and skew estimation for the symmetric exponential model delay was proposed by Chaudhari [11]. However, the previously proposed estimation methods are very sensitive to changes in the network delay distribution. Recently, Kim et al. [4] developed a robust estimation scheme for clock offset called the Gaussian Mixture Kalman Particle Filtering (GMKPF), and which was shown to provide better performance for arbitrary network delay distributions relative to MLE. Drawbacks of the study undertaken by Kim et al. [4] are the facts that analytical closed form expressions for MSE do not necessarily exist and that lower bounds are hard to derive.

While significant progress has been made in the effort to efficiently estimate clock offset and skew, estimation schemes which are not sensitive to non-Gaussian/non-exponential network delays have not been developed yet. This research, therefore, will

conduct a series of computer simulation to assess the performance of GMKPF in estimating both the clock offset and skew parameters.

1.4 Problem Description

The clock offset and skew parameters are two factors that determine the accuracy and guarantee long-term reliability of time synchronization in WSNs, and therefore, reduction of network energy consumption which is the key strategy in obtaining energy efficiency usage.

Clock synchronization between any two nodes is generally accomplished by message exchanges. Due to the presence of non-deterministic message delays, messages can get delay arbitrarily. It is important to develop an estimator which performs well in any network delay environment.

As depicted later in Chapter II, in the Figure on page 11, the clock offset and skew measurement is modeled as equation on page 11. In order to obtain a robust estimation scheme for clock offset and skew, GMKPF was first studied and the MSE performance of GMKPF was compared with the MSE performance of GMLE and EMLE through computer simulations. Then, GMKPF was used to estimate the clock offset and skew parameters by formulating the problem as described in Section 2.7. A series of computer simulations was conducted in order to verify the MSE performance of GMKPF through comparisons with JMLE and MLLE.

1.5 Research Objective

This research aims at two main objectives:

- Study the previously proposed clock offset and joint clock offset and skew parameter estimation methods: MLE, JMLE, MLLE, and GMKPF.
- Conduct a computer simulation to study the robustness of the clock offset and skew estimation scheme based on GMKPF assuming Gaussian and general non-Gaussian delay distributions such as exponential, Gamma, and Weibull and compare their MSE performance with that of JMLE and MLLE.

By achieving the above goals, this research was able to provide a robust clock synchronization method by estimating both the clock offset and skew parameters.

CHAPTER II

SYSTEM DESCRIPTION AND BACKGROUND THEORIES

2.1 Two-way Message Exchange Mechanism Without Clock Skew

Assuming no clock skew, a number of N two-way message exchanges or sender-receiver synchronization (SRS) exchanges are graphically shown in Figure 2.1. $T_{1,k}$ and $T_{4,k}$ represent the timestamps measured by the local clock of node A, while $T_{2,k}$ and $T_{3,k}$ represent the timestamps measured by the local clock of node B at the k^{th} message exchange.

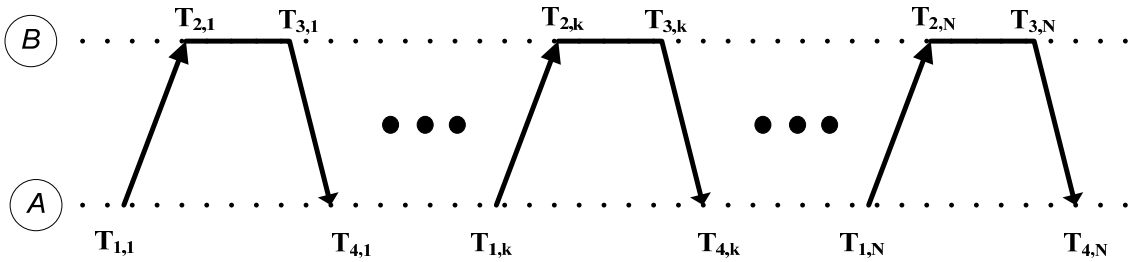

Figure 2.1: Two-way message exchange mechanism which assumes only clock offset

Based on the above pairwise message exchange mechanism, the clock offset measurement model can be represented in terms of the following two equations [8]:

$$\begin{aligned} T_{2,k} &= T_{1,k} + d + \phi + X_k, \\ T_{4,k} &= T_{3,k} + d - \phi + Y_k, \end{aligned} \tag{2.1}$$

where d denotes the fixed portions of the delay, and ϕ represents the clock offset between node A and node B. X_k and Y_k denote the variable portions of delay.

The equation (2.1) can also be rewritten as

$$\begin{aligned} U_k &= d + \phi + X_k, \\ V_k &= d - \phi + Y_k, \end{aligned} \tag{2.2}$$

where the time differences U_k and V_k corresponding to the k^{th} uplink and downlink message exchange, are defined as $U_k \triangleq T_{2,k} - T_{1,k}$ and $V_k \triangleq T_{4,k} - T_{3,k}$ respectively.

2.2 Maximum Likelihood Clock Offset Estimation

Delay measurements in equation (2.2) produce a MLE of the clock offset when the fixed delays in each direction are equal and the variable delays in each direction assume the same distribution, namely Gaussian or exponential distribution.

2.2.1 Gaussian Delay Model

Assuming the symmetric Gaussian delay for uplink and downlink, the set of delay observations $\{X_k\}_{k=1}^{N}$ and $\{Y_k\}_{k=1}^{N}$ are independent and normally distributed with the same mean μ and variance σ^2. The likelihood function based on the observations $\{U_k\}_{k=1}^{N}$ and $\{V_k\}_{k=1}^{N}$ is given by [8]

$$L(\phi, \mu, \sigma^2) = (2\pi\sigma^2)^{-N} \exp\{-\frac{1}{2\sigma^2}[\sum_{k=1}^{N}(U_k - d - \phi - \mu)^2 + \sum_{k=1}^{N}(V_k - d + \phi - \mu)^2]\}. \tag{2.3}$$

Differentiating the log-likelihood function gives

$$\frac{\partial \ln L(\phi)}{\partial \phi} = -\frac{1}{\sigma^2}[\sum_{k=1}^{N} 2\phi - (U_k - V_k)]. \tag{2.4}$$

Hence, the MLE of clock offset is given by

$$\frac{\partial \ln L(\hat{\phi}_{GMLE})}{\partial \hat{\phi}_{GMLE}} = -\frac{1}{\sigma^2}[\sum_{k=1}^{N} 2\hat{\phi}_{GMLE} - (U_k - V_k)] = 0$$

$$\hat{\phi}_{GMLE} = \frac{\sum_{k=1}^{N}(U_k - V_k)}{2N} = \frac{\bar{U} - \bar{V}}{2}. \tag{2.5}$$

2.2.2 Exponential Delay Model

Assuming the symmetric exponential delay model for the uplink and downlink, the set of delay observations $\{X_k\}_{k=1}^{N}$ and $\{Y_k\}_{k=1}^{N}$ are independent and exponentially distributed with the same mean α. $\{U_k\}_{k=1}^{N}$ and $\{V_k\}_{k=1}^{N}$ define the order statistics of the sequences of observations $\{U_k\}_{k=1}^{N}$ and $\{V_k\}_{k=1}^{N}$, respectively. The likelihood function based on the observations is given by [9]

$$\begin{aligned} L(d,\phi,\alpha) = \alpha^{-2N} \exp\{-[\sum_{k=1}^{N} U_k + \sum_{k=1}^{N} V_k - 2Nd]\} \\ \times I[U_{(1)} \geq d + \phi, V_{(1)} \geq d - \phi]. \end{aligned} \tag{2.6}$$

MLE of clock offset is given by [9]

$$\hat{\phi}_{EMLE} = \frac{U_{(1)} - V_{(1)}}{2}. \tag{2.7}$$

2.3 Two-way Message Exchange Mechanism with Clock Offset and Skew

Due to the imperfections of the clock oscillator, the clock of each node presents different clock offsets and skews. Moreover, the clock offset between two nodes actually keeps increasing because of the effect of clock skew. Therefore, a fixed value model or

equation (2.1) for clock offset is not sufficient for practical situations. As a consequence, estimating the clock offset and skew will increase the accuracy and maintain long-term reliability of synchronization.

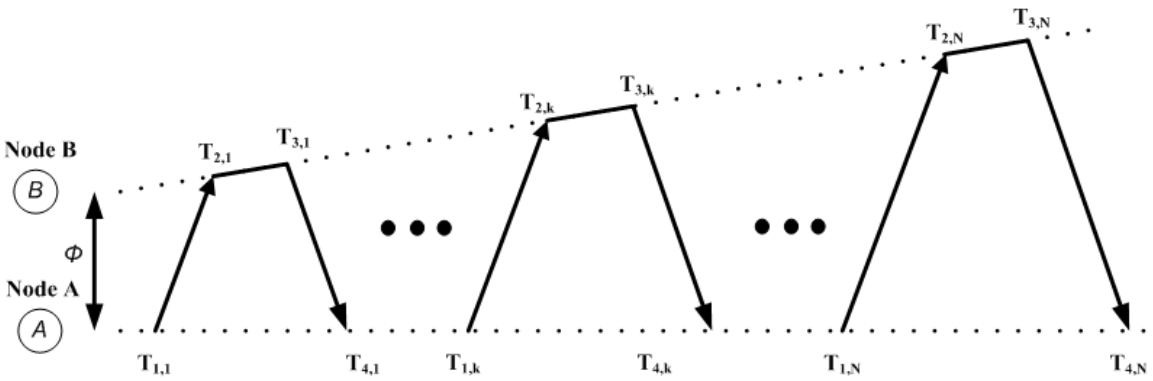

Figure 2.2: Two-way message exchange mechanism assuming both clock offset and skew.

The effect of clock offset and skew are depicted in Figure 2.2. Here, the timestamps in the k^{th} message exchange $T_{1,k}$ and $T_{4,k}$ are measured at node A, and $T_{2,k}$ and $T_{3,k}$ are measured at node B. Assuming $T_{1,1}$ is set to zero and it serves as the reference time, the clock offset and skew measurement could be modeled as [1]

$$\begin{aligned} T_{2,k} &= (T_{1,k} + d + X_k)\omega + \phi, \\ T_{3,k} &= (T_{4,k} - d - Y_k)\omega - \phi, \end{aligned} \tag{2.8}$$

where ω represents the clock skew parameter.

2.4 Joint Maximum Likelihood Estimation (JMLE) of Clock Offset and Skew

The theory applied thus far for finding the MLE for the clock offset (assuming no clock skew) can be extended to find JMLE for a more general clock model (2.8).

2.4.1 Gaussian Delay Model

Assume $\{X_k\}_{k=1}^N$ and $\{Y_k\}_{k=1}^N$ are zero mean independent Gaussian distributed random variables with variance σ^2 and the fixed portion of delay *d* is known. The JMLE of clock offset and skew based on the observations $\{T_{1,k}\}_{k=1}^N$, $\{T_{2,k}\}_{k=1}^N$, $\{T_{3,k}\}_{k=1}^N$, and $\{T_{4,k}\}_{k=1}^N$ is given by [1]

$$\hat{\phi}_{GMLE} = \frac{\sum_{k=1}^{N}(T_{1,k}+T_{4,k})\sum_{k=1}^{N}(T_{2,k}{}^2+T_{3,k}{}^2)-\sum_{k=1}^{N}(T_{2,k}+T_{3,k})Q}{\sum_{k=1}^{N}(T_{2,k}+T_{3,k})\sum_{k=1}^{N}(T_{1,k}+T_{4,k})-2NQ}, \tag{2.9}$$

$$\begin{aligned}\hat{\omega}_{GMLE} = {} & \frac{-2N[\sum_{k=1}^{N}(T_{1,k}+T_{4,k})\sum_{k=1}^{N}(T_{2,k}{}^2+T_{3,k}{}^2)-\sum_{k=1}^{N}(T_{2,k}+T_{3,k})Q]}{\sum_{k=1}^{N}(T_{1,k}+T_{4,k})[\sum_{k=1}^{N}(T_{2,k}+T_{3,k})\sum_{k=1}^{N}(T_{1,k}+T_{4,k})-2NQ]} \\ & + \frac{\sum_{k=1}^{N}(T_{2,k}+T_{3,k})}{\sum_{k=1}^{N}(T_{1,k}+T_{4,k})},\end{aligned} \tag{2.10}$$

where $Q \triangleq \sum_{k=1}^{N}[T_{1,k}T_{2,k}+T_{3,k}T_{4,k}+(T_{2,k}-T_{3,k})d]$.

2.4.2 Exponential Delay Model

Assuming the symmetric exponential delay model for the uplink and downlink then the set of delay observations $\{X_k\}_{k=1}^N$ and $\{Y_k\}_{k=1}^N$ are independently and exponentially distributed with the same mean α**.** In paper [11], the authors assumed that α is known and categorized JMLE of clock offset and skew into four cases:

Case I: d known, ϕ known;

Case II: d unknown, ϕ known;

Case III: d known, ϕ unknown;

Case IV: d unknown, ϕ unknown.

This thesis studies the MSE performance in the case that the fixed portion delay, d is known, ϕ unknown and ω unknown. The algorithm for finding $\hat{\phi}$ and $\hat{\omega}$ when d is known is given by the following operations:

1. $$\textit{Find} \quad \phi^{k,l} = \frac{T_{3,l}(T_{1,k}+d) - T_{2,k}(T_{4,l}-d)}{(T_{1,k}+d)-(T_{4,l}-d)};$$
$$\omega^{k,l} = \frac{T_{2,k}-T_{3,l}}{(T_{1,k}+d)-(T_{4,l}-d)}; \qquad (2.11)$$
$$\forall k = 1,...,N \quad \textit{and} \quad \forall l = 1,...,N;$$

2. $$(i,j) = \{(k,l) \mid \omega^{k,l} \le \frac{T_{2,r}-\phi^{k,l}}{T_{1,r}+d} \textit{ and } \omega^{k,l} \ge \frac{T_{3,r}-\phi^{k,l}}{T_{4,r}-d}\}; \qquad (2.12)$$
$$\forall r = 1,...,N;$$

3. $$(m,n) = \{(k,l) \mid (k,l) \ne (i,j), \omega^{k,l} \le \frac{T_{2,r}-\phi^{k,l}}{T_{1,r}+d} \textit{ and } \omega^{k,l} \ge \frac{T_{3,r}-\phi^{k,l}}{T_{4,r}-d}\}; \qquad (2.13)$$
$$\forall r = 1,...,N;$$

4. $$\hat{\omega}_{EMLE} = \min\{\omega^{i,j}, \omega^{m,n}\}; \quad \hat{\phi}_{EMLE} = \max\{\phi^{i,j}, \phi^{m,n}\}; \qquad (2.14)$$

2.5 Maximum Likelihood-Like Estimator (MLLE)

Figure 2.2 shows that the clock difference between two nodes is monotonically increasing based on the linear clock skew model in equation (2.8). The largest clock difference is between the first and last time stamps. From this intuition, MLLE is

proposed in [8] based on the information provided solely by the first and the last timestamps.

Define the distances of the first and last time stamps as $D_{(1)} \triangleq T_{1,N} - T_{1,1}$, $D_{(2)} \triangleq T_{2,N} - T_{2,1}$, $D_{(3)} \triangleq T_{3,N} - T_{3,1}$, and $D_{(4)} \triangleq T_{4,N} - T_{4,1}$. From (2.8), subtracting $T_{2,1}$ from $T_{2,N}$ and subtracting $T_{4,1}$ from $T_{4,N}$ yields

$$T_{2,N} - T_{2,1} = (T_{1,N} - T_{1,1} + X_N - X_1)\omega,$$
$$T_{3,N} - T_{3,1} = (T_{4,N} - T_{4,1} + Y_1 - Y_N)\omega,$$

which can be further rewritten as

$$D_{(2)} = (D_{(1)} + X_N - X_1)\omega,$$
$$D_{(3)} = (D_{(4)} - (Y_N - Y_1))\omega. \qquad (2.15)$$

2.5.1 Gaussian Delay Model

In the Gaussian delay model, X_1, X_N, Y_1, and Y_N are independent and identically normally distributed random variables with zero mean and variance σ^2. Therefore, X_N - X_1 and Y_N - Y_1 are normally distributed random variables with zero mean and variance $2\sigma^2$.

Define X_N - X_1 as the variable P and Y_N - Y_1 as the variable R. Then the joint pdf of P and R is given by

$$f_{P,R}(p,r) = \frac{1}{4\pi\sigma^2} \exp[-\frac{1}{4\sigma^2}(p^2 + r^2)].$$

Thus, the likelihood function based on model (2.15) is

$$L(\omega,\sigma^2)=\frac{1}{4\pi\sigma^2}\exp\left\{-\frac{1}{4\sigma^2}\left[D_{(2)}^2(\frac{1}{\omega}-\frac{D_{(1)}}{D_{(2)}})^2+D_{(3)}^2(\frac{1}{\omega}-\frac{D_{(4)}}{D_{(3)}})^2\right]\right\}.$$

Define $\omega' \triangleq 1/\omega$ and differentiating the log-likelihood function with respect to ω' yields

$$\frac{\partial \ln L(\omega',\sigma^2)}{\partial\omega'}=-\frac{1}{2\sigma^2}\left[D_{(2)}^2(\omega'-\frac{D_{(1)}}{D_{(2)}})^2+D_{(3)}^2(\omega'-\frac{D_{(4)}}{D_{(3)}})^2\right],$$

$$\frac{\partial \ln L(\hat{\omega}',\sigma^2)}{\partial\hat{\omega}'}=0=-\frac{1}{2\sigma^2}\left[D_{(2)}^2(\hat{\omega}'-\frac{D_{(1)}}{D_{(2)}})+D_{(3)}^2(\hat{\omega}'-\frac{D_{(4)}}{D_{(3)}})\right],$$

$$\hat{\omega}'=\frac{D_{(1)}D_{(2)}+D_{(3)}D_{(4)}}{D_{(2)}^2+D_{(3)}^2}.$$

Thus, the MLLE for the Gaussian delay model (GMLLE) is given by:

$$\hat{\omega}_{GMLLE}=\frac{D_{(2)}^2+D_{(3)}^2}{D_{(1)}D_{(2)}+D_{(3)}D_{(4)}}. \tag{2.16}$$

Then, we could express the clock offset estimator as follows:

$$\hat{\phi}_{GMLLE}=\frac{\bar{U}_k'-\bar{V}_k'}{2}, \tag{2.17}$$

where $U_k'=T_{2,k}-\hat{\omega}_{GMLLE}T_{1,k}$ and $V_k'=\hat{\omega}_{GMLLE}T_{4,k}-T_{3,k}$.

2.5.2 Exponential Delay Model

In the exponential delay model, X_1, X_N, Y_1, and Y_N are independent and identically distributed normal random variables with the same mean, and X_N - X_1 and Y_N - Y_1 are normally distributed random variables with zero mean. Similarly to the Gaussian delay model, X_N - X_1 is defined as the variable P and Y_N - Y_1 is defined as the variable R. P

and R are zero mean Laplace distributed random variables with variance $2\alpha^2$ and the joint pdf of P and R is given by

$$f_{P,R}(p,r)=\left(\frac{1}{2\alpha}\right)^2 \exp[-\frac{1}{\alpha}(|\,p\,|+|\,r\,|)].$$

The likelihood function based on model (2.15) is

$$L(\omega,\alpha)=\left(\frac{1}{2\alpha}\right)^2 \exp\left[-\frac{1}{\alpha}\left(|\,\frac{D_{(2)}}{\omega}-D_{(1)}\,|+|\,D_{(4)}-\frac{D_{(3)}}{\omega}\,|\right)\right].$$

Substituting $\omega' \triangleq 1/\omega$, the likelihood function can be rewritten as

$$L(\omega',\alpha)=\left(\frac{1}{2\alpha}\right)^2 \exp\left[-\frac{1}{\alpha}\left(|\,D_{(2)}\omega'-D_{(1)}\,|+|\,D_{(4)}-D_{(3)}\omega'\,|\right)\right].$$

The maximization of the likelihood function is reduced to

$$\hat{\omega}'=\arg\min_{\omega'}(|\,D_{(2)}\omega'-D_{(1)}\,|+|\,D_{(4)}-D_{(3)}\omega'\,|). \tag{2.18}$$

Therefore, the MLLE of the exponential delay model (EMLLE) is given by;

$$\hat{\omega}_{EMLLE}=\begin{cases}\dfrac{D_{(2)}}{D_{(1)}}, & D_{(2)}>D_{(3)}\\[2ex] \dfrac{D_{(3)}}{D_{(4)}}, & D_{(2)}<D_{(3)}\\[2ex] \dfrac{1}{2}\left(\dfrac{D_{(2)}}{D_{(1)}}+\dfrac{D_{(3)}}{D_{(4)}}\right), & D_{(2)}=D_{(3)}\end{cases}. \tag{2.19}$$

Then, we could express the clock offset estimator as

$$\hat{\phi}_{EMLLE}=\frac{\min_{1\le k\le N}U_k^{'}-\min_{1\le k\le N}V_k^{'}}{2}, \tag{2.20}$$

where $U_k^{'}=T_{2,k}-\hat{\omega}_{EMLLE}T_{1,k}$ and $V_k^{'}=\hat{\omega}_{EMLLE}T_{4,k}-T_{3,k}$.

2.6 Clock Offset Estimation Based on the Gaussian Mixture Kalman Particle Filter

Gaussian Mixture Kalman Particle Filter (GMKPF) provides a scheme which is robust to arbitrary random delay distributions such as asymmetric Gaussian, asymmetric exponential, Gamma, Weibull, as well as to mixtures of these delay models for estimating the clock offset in WSNs. In addition, an advantage of GMKPF is in terms of its superior performance as compared to GMLE and EMLE.

2.6.1 Problem Modeling

In this section, the two-way message exchange mechanism is represented by a set of state-space and observation equations, called a dynamic state-space model (DSSM), as depicted in Figure 2.3. The observations y_k are conditionally independent given the state and are generated according to the probability density $p(y_k \mid x_k)$. The state x_k evolves over time as an unobserved first order Markov process according to the probability density $p(x_k \mid x_{k-1})$. The DSSM can be described via the set of equations:

$$x_k = f(x_{k-1}, v_{k-1}) \quad (process\ equation), \tag{2.21}$$

$$y_k = h(x_k, n_k) \quad (observation\ equation), \tag{2.22}$$

where v_k is the process noise of state transition function f, and n_k is the observation noise of observation function h.

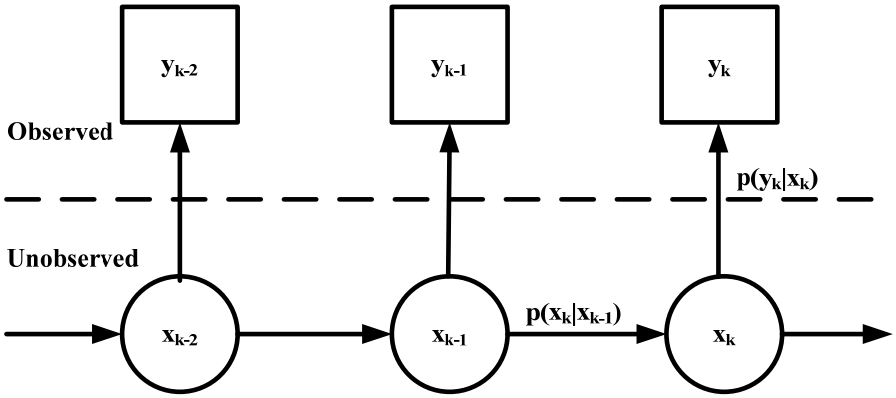

Figure 2.3: Dynamic state space model.

Based on the clock synchronization model (2.2) from Section 2.1, the unknown clock offset ϕ's behavior follows a Gauss-Markov dynamic channel model of the form:

$$\phi_{k+1} = A\phi_k + v_k, \tag{2.23}$$

where A represents the state transition matrix for the clock offset. The noise vector v_k is modeled as a Gaussian random variable with zero mean and covariance $E[v_k v_k^T] = Q$.

The uplink delay U_k and downlink delay V_k of the k^{th} timing message exchange can be observed at node A and node B. The vector of observations $z_k = [U_k \; V_k]^T$ can be expressed as in the observation equation (2.22),

$$z_k = \begin{bmatrix} U_k \\ V_k \end{bmatrix} = \begin{bmatrix} d + \phi_k + X_k \\ d - \phi_k + Y_k \end{bmatrix} = \begin{bmatrix} 1 \\ 1 \end{bmatrix} d + \begin{bmatrix} 1 \\ -1 \end{bmatrix} \phi_k + n_k, \tag{2.24}$$

where the observation noise vector is $n_k = [X_k \; Y_k]^T$. X_k and Y_k may assume any distribution such as Gaussian, exponential, Gamma, Weibull or a mixture of two distributions.

Given all the observation samples $Z_k = \{z_1, z_2, \ldots, z_k\}$, the goal is to find the minimum MSE estimator of the unknown clock offset ϕ_k, which is given by

$$\hat{\phi}_k = E[\phi_k \mid Z_k] = \int \phi_k \, p(\phi_k \mid Z_k) d\phi_k .$$

The optimal method to recursively update the posterior density as new observations arrive is given by the recursive Bayesian estimation algorithm

$$p(\phi_k \mid Z_k) = C p(z_k \mid \phi_k) \, p(\phi_k \mid Z_{k-1}),$$

where $$p(\phi_k \mid Z_{k-1}) = \int p(\phi_k \mid \phi_{k-1}) \, p(\phi_{k-1} \mid Z_{k-1}) d\phi_{k-1}$$

and $$C = \left(\int p(z_k \mid \phi_k) \, p(\phi_k \mid Z_{k-1}) d\phi_k \right)^{-1} .$$

However, the expression of $p(x_k \mid Z_k)$ can be obtained in closed-form expression only for the case of a linear Gaussian model. In equation (2.24), X_k and Y_k could be non-Gaussian distributions, consequently, $p(x_k \mid Z_k)$ cannot be analytically obtained. Alternatively, $p(x_k \mid Z_k)$ can be recursively approximated via particle filtering.

2.6.2 Framework of GMKPF

Particle filtering is a sequential Monte Carlo methodology [12] where the basic idea is the recursive computation of relevant probability distributions using the concepts of importance sampling (IS) and approximation of probability distributions with discrete random measures. GMKPF in [4] is developed based on the Gaussian mixture sigma point particle filter (GMSPPF) proposed in [13]. The GMSPPF combines an IS based measurement update step with a Sigma-Point Kalman Filter (SPKF) [14] based on the

Gaussian sum filter [15] for the time update and proposal density function. Since the DSSM of clock synchronization explained in the previous section is a linear model, GMKPF implements the Kalman Filter (KF) [16] instead of SPKF. The framework of GMKPF mainly relies on these three elements:

1) Gaussian mixture model (GMM) approximation

Any probability $p(x)$ can be approximated as closely as desired by a Gaussian mixture model (GMM) of the following form:

$$p(x) \approx p_g(x) = \sum_{g=1}^{G} \alpha^{(g)} N(x; \mu^{(g)}, P^{(g)}), \tag{2.25}$$

where G stands for the number of mixing components, $\alpha^{(g)}$ are the mixing weights and $N(x; \mu, P)$ denotes the normal distribution with mean vector μ and positive definite covariance P. For example, the following density function can be approximated by GMMs:

$$\textit{posterior density},\ p(x_k \mid Z_k) \approx p_g(x_k \mid Z_k) = \sum_{g''=1}^{G''} \alpha^{(g'')} N(x; \mu_k^{(g'')}, P_k^{(g'')}).$$

The predicted and updated Gaussian component mean and covariance of $p_g(x_k \mid Z_k)$ are calculated using KF.

2) Importance sampling (IS) based measurement update

In particle filtering, the distributions are approximated by discrete random measures defined by particles and weights assigned to the particles. If the distribution of interest is $p(x)$ and its approximating random measure is $\chi = \{x^{(m)}, w^{(m)}\}_{m=1}^{M}$, where $x^{(m)}$ are the

particles, $w^{(m)}$ are the corresponding weights, and M denotes the number of particles used in the approximation, then $p(x)$ is approximated by [12]

$$p(x) \approx \sum_{m=1}^{M} w^{(m)} \delta(x - x^{(m)}),$$

where $\delta(\bullet)$ is the Dirac delta function. With this approximation, computations of expectations are simplified and approximated by [12]

$$E(g(x)) \approx \sum_{m=1}^{M} w^{(m)} g(x^{(m)}).$$

Based on DSSM model (2.23) and (2.24), the conditional mean state and corresponding error covariance are calculated as follows:

$$\bar{\phi}_k = \sum_{m=1}^{M} w_k^{(m)} \phi_k^{(m)}, \tag{2.26}$$

$$\bar{P}_k = \sum_{m=1}^{M} w_k^{(m)} [\bar{\phi}_k - \phi_k^{(m)}][\bar{\phi}_k - \phi_k^{(m)}]^T. \tag{2.27}$$

The updated importance weights can be obtained by [13]

$$w_k^{(m)} = w_{k-1}^{(m)} \frac{p(z_k \mid \phi_k^{(m)}) p(\phi_k^{(m)} \mid \phi_{k-1}^{(m)})}{\pi(\phi_k^{(m)} \mid \phi_{0:k-1}^{(m)}, z_{0:k})}.$$

The distribution $\pi(\phi_k^{(m)} \mid \phi_{0:k-1}^{(m)}, z_{0:k})$ is known as an importance function. In GMKPF, the proposal distribution for $\pi(\phi_k^{(m)} \mid \phi_{0:k-1}^{(m)}, z_{0:k})$ is approximated by GMM from the bank of KFs. By sampling the particles from such a distribution will move the particles to areas of high likelihood which in turn resolves the sample depletion problem of particle filtering. Moreover, using the GMM approximation on the predictive posterior density function preserves the kernel smoothing nature.

3) Weighted EM for resampling and GMM recovery

In standard particle filtering, resampling is needed in order to keep good performance of particle filter. Resampling is a scheme that discards particles which are assigned negligible weights and replicates particles with large weights [12]. Unfortunately, resampling causes particle depletion in cases where the measurement likelihood is very high. Consequently, the set of particles will be only copies of the same particle [17]. In GMKPF, the posterior density is represented by GMM; hence, the standard resampling method can be replaced by a weighted Expectation-Maximization (EM) algorithm [18]. It directly recovers a maximum-likelihood G-component GMM fit to the set of weighted samples; as a result, it prevents the particle depletion problem. The EM algorithm provides an iterative method of estimating $\bar{\theta}$ via

$$\bar{\theta} = \arg\max_{\theta} p(z \mid \theta).$$

The G-component GMM is specified by the parameter set

$$\theta = \{\alpha_k^{(1)}, ..., \alpha_k^{(G)}, \mu_k^{(1)}, ..., \mu_k^{(G)}, P_k^{(1)}, ..., P_k^{(G)}\}.$$

The EM algorithm represents a two-step iterative algorithm which is described by the following two steps:

- $E\ step: Q(\theta \mid \theta^{(j)}) = E[\log p(z \mid \theta) \mid \theta^{(j)}]$,
- $M\ step: \theta^{(j+1)} = \arg\max_{\theta} Q(\theta \mid \theta^{(j)})$.

Finally, the conditional mean state estimate and corresponding error covariance are calculated as follows:

$$\bar{\phi}_k = \sum_{g=1}^{G} \alpha_k^{(g)} \mu_k^{(g)},$$

$$\bar{P}_k = \sum_{g=1}^{G} \alpha_k^{(g)} \left[P^{(g)}_k + (\mu_k^{(g)} - \bar{\phi}_k)(\mu_k^{(g)} - \bar{\phi})^T \right].$$

2.6.3 GMKPF Algorithm

In this section, the full GMKPF algorithm will be presented based on the framework described in the previous section.

1) Time update and proposal distribution generation

1.1) At time $k-1$, initialize the state densities:

- The posterior state density is approximated by

$$p_g(\phi_{k-1} \mid Z_{k-1}) = \sum_{g=1}^{G} \alpha_{k-1}^{(g)} N(\phi_{k-1}; \mu_{k-1}^{(g)}, P_{k-1}^{(g)});$$

- The process noise density is approximated by

$$p_g(v_{k-1}) = \sum_{i=1}^{I} \beta_{k-1}^{(i)} N(v_{k-1}; \mu_{v_{k-1}}^{(i)}, P_{v_{k-1}}^{(i)});$$

- The observation noise density is approximated by

$$p_g(n_k) = \sum_{j=1}^{J} \gamma_k^{(j)} N(n_k; \mu_{n_k}^{(j)}, P_{n_k}^{(j)}).$$

1.2) During the time update step of KF (employing the system process equation (2.23), posterior state density $p_g(\phi_{k-1} \mid Z_{k-1})$ and process noise density $p_g(v_{k-1})$ from above), a Gaussian approximated predictive state

density $\hat{p}_g(\phi_k \mid Z_{k-1}) = \sum_{g'=1}^{G'} \alpha_k^{(g')} N(\phi_k; \hat{\mu}_k^{(g')}, \hat{P}_k^{(g')})$ is calculated. The Gaussian approximated posterior state density,

$$\hat{p}_g(\phi_k \mid Z_k) = \sum_{g''=1}^{G''} \alpha_k^{(g'')} N(\phi_k; \mu_k^{(g'')}, P_k^{(g'')}),$$

is calculated during the measurement update step of KF (employing the system observation equation (2.24), current observation z_k pre-predictive state density $\hat{p}_g(\phi_k \mid Z_{k-1})$ and observation noise density $p_g(n_k)$).

2) Measurement update

2.1) Draw M samples $\{\phi_k^{(m)}; m = 1, ..., M\}$ from the importance density function $\hat{p}_g(\phi_k \mid Z_k)$.

2.2) Calculate the corresponding importance weights:

$$\tilde{w}_k^{(m)} = \frac{p(z_k \mid \phi_k^{(m)}) \hat{p}_g(\phi_k^{(m)} \mid Z_{k-1})}{\hat{p}_g(\phi_k^{(m)} \mid Z_k)}.$$

2.3) Normalize the weights $w_k^{(m)} = \frac{\tilde{w}_k^{(m)}}{\sum_{m=1}^{M} \tilde{w}_k^{(m)}}$.

2.4) Use a weighted EM algorithm to fit a G-component GMM to the set of weighted particles $\{w_k^{(m)}, \phi_k^{(m)}; m = 1, ..., M\}$, which represent the update GMM approximate state posterior distribution at time k, $p_g(\phi_k \mid Z_k)$.

3) Inference of the conditional mean and covariance

3.1) $\bar{\phi}_k = \sum_{m=1}^{M} w_k^{(m)} \phi_k^{(m)}$ and $\bar{P}_k = \sum_{m=1}^{M} w_k^{(m)} [\bar{\phi}_k - \phi_k^{(m)}][\bar{\phi}_k - \phi_k^{(m)}]^T$ or equivalently, upon fitting the GMM approximate posterior distribution through the weighted EM algorithm, calculate the conditional mean state estimate and corresponding error covariance.

2.7 Joint Clock Offset and Skew Estimation Based on GMKPF

In this section, a robust scheme for estimation of clock offset and skew in wireless sensor networks is designed based on GMKPF. The only difference is the process equation and observation equation of state space model which will be described in Section 2.7.1.

2.7.1 Problem Modeling

Consider the clock offset and skew model (2.8); described by the equation

$$T_{2,k} = (T_{1,k} + d + X_k)\omega + \phi,$$
$$T_{3,k} = (T_{4,k} - d - Y_k)\omega - \phi.$$

Let θ_B be defined as $\omega - 1$. Then, the model above can be rewritten as;

$$\begin{aligned} T_{2,k} - T_{1,k} &= U_k = (d + X_k)(1 + \theta_B) + \theta_B T_{1,k} + \phi, \\ T_{4,k} - T_{3,k} &= V_k = (d + Y_k)(1 + \theta_B) - \theta_B T_{4,k} - \phi. \end{aligned} \tag{2.28}$$

Assuming, the unknown ϕ and θ_B obey a Gauss-Markov dynamic channel model of the form:

$$\begin{bmatrix} \phi_{k+1} \\ \theta_{B,k+1} \end{bmatrix} = A \begin{bmatrix} \phi_k \\ \theta_{B,k} \end{bmatrix} + v_k$$
$$x_{k+1} = Ax_k + v_k \tag{2.29}$$

where A represents the state transition matrix and $x_k = [\phi_k \quad \theta_{B,k}]^T$. The noise vector v_k is modeled as a Gaussian random variable with zero mean and covariance $E[v_k v_k^T] = Q$. Based on observation model (2.28), the observation equation can be written as

$$\begin{aligned} z_k = \begin{bmatrix} U_k \\ V_k \end{bmatrix} &= \begin{bmatrix} (d + X_k)(1+\theta_{B,k}) + \theta_{B,k} T_{1,k} + \phi_k \\ (d + Y_k)(1+\theta_{B,k}) - \theta_{B,k} T_{4,k} - \phi_k \end{bmatrix} \\ &= \begin{bmatrix} \theta_{B,k} & 0 \\ 0 & -\theta_{B,k} \end{bmatrix} C_k + \begin{bmatrix} 1+\theta_{B,k} \\ 1+\theta_{B,k} \end{bmatrix} d + \begin{bmatrix} 1 \\ -1 \end{bmatrix} \phi_k + (1+\theta_{B,k}) n_k, \end{aligned} \tag{2.30}$$

where the observation noise vector $n_k = [X_k \; Y_k]^T$. X_k and Y_k may assume any distribution such as Gaussian, exponential, Gamma, Weibull or a mixture of two distributions. $C_k = [T_{1,k} \; T_{4,k}]^T$ is treated as exogenous input to the state observation function. In short, we can write equation (2.30) as $z_k = h(\phi_k, \theta_{B,k}, C_k)$ where $h(\bullet)$ is the state observation function. In Figure 2.4 is depicted a DSSM model for clock offset and skew estimation method based on GMKPF.

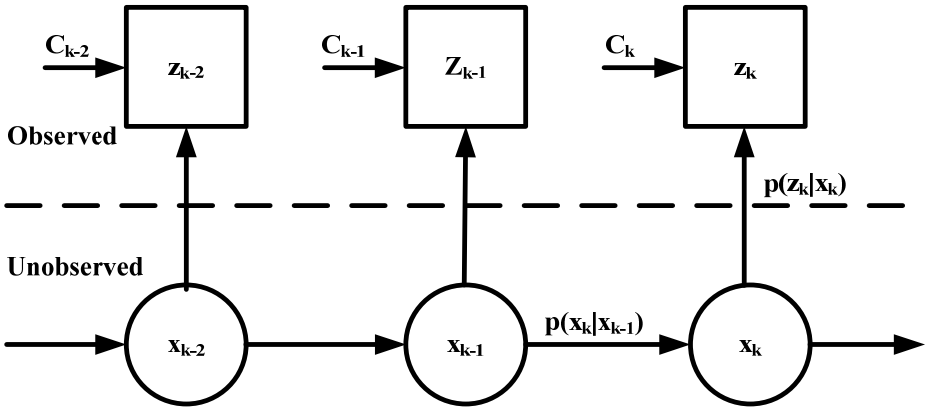

Figure 2.4: Dynamic state space model of clock offset and skew.

CHAPTER III

PERFORMANCE OF GMKPF

3.1 Clock Offset Estimation Based on GMKPF

In this section, computer simulation results will be presented to determine the performance of GMKPF (Section 2.6), GMLE and EMLE (Section 2.2) methods for estimating the clock offset in WSNs. The observation noise delay models are considered to be twelve delay distributions: symmetric Gaussian, symmetric exponential, asymmetric Gaussian, asymmetric exponential, Gamma, Weibull and mixtures of Gaussian and exponential, Gaussian and Gamma, Gaussian and Weibull, exponential and Gamma, exponential and Weibull, and Gamma and Weibull. The number of Monte Carlo simulations is 2000. The state transition matrix A of process equation is 0.99999. The process noise v_k is assumed to be Gaussian with constant covariance, Q = 1e-5. The number of particles and GMM components are 1000 and 5, respectively. The experiment was done using Matlab and ReBEL Toolkit[1].

Figure 3.1 shows a plot of the clock offset estimation in each Monte Carlo simulation. The MSE performances of estimators are averaged over 2000 Monte Carlo runs. Figures A.1-A.12 show the MSEs of the estimators assuming that the random delay models are symmetric Gaussian, exponential, asymmetric Gaussian, exponential, Gamma, and Weibull distributions, and mixtures of two distributions respectively.

[1] ReBEL is a Matlab toolkit for sequential Bayesian inference in General DSSMs. ReBEL is developed by MLSP Group at OGI and can be freely downloaded from http://cslu.ece.ogi.edu/mslp/rebel for academic and /or non-commercial use.

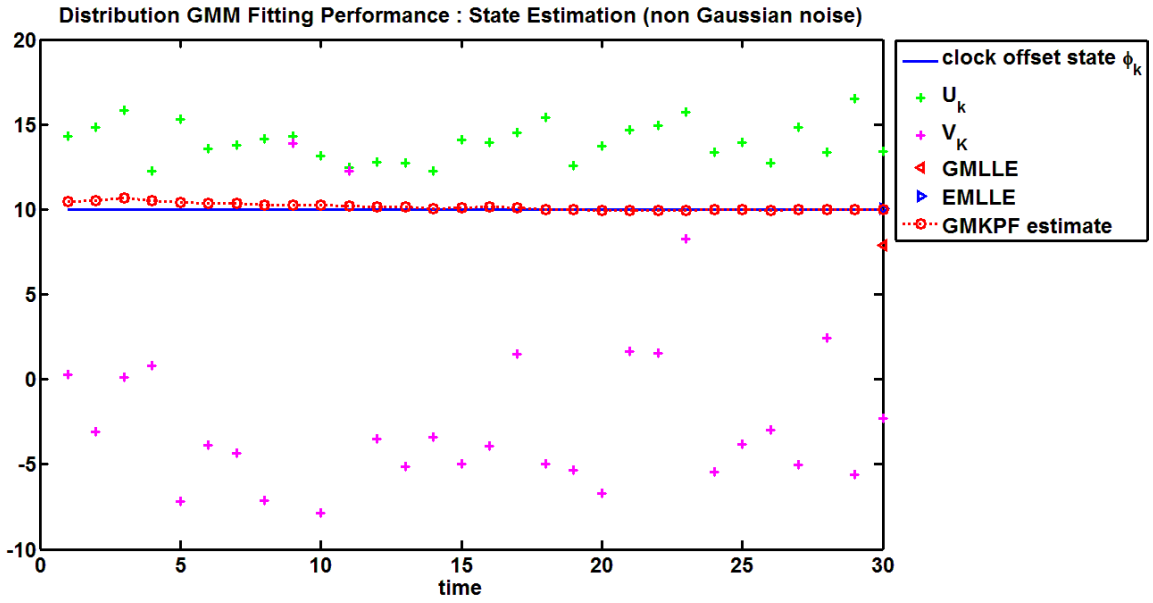

Figure 3.1: Clock offset state estimation via GMKPF.

The subscripts 1 and 2 are used to differentiate between the parameters of delay distributions corresponding to the uplink and the downlink, respectively. For example, in Figure A.3, the parameters σ_1 and σ_2 are standard deviations of uplink and downlink assuming Gaussian delay distributions, respectively. The number of observations which are experimented in the simulation are 10, 15, 20, 25 and 30. To construct a mixing noise delay distribution, two distributions are mixed with equal weight. For example, a Gaussian delay and exponential delay are generated and mixed with an equal weight of 50%. The number of observations which are experimented for the mixing case is 10, 16, 22, and 28, respectively.

From Figures A.1-A.12, GMKPF clearly outperforms GMLE and EMLE, and results in reduction of MSE over 100%. GMLE performs better than EMLE in the presence of Gaussian random delays (Figures A.1, A.3, A.7 and A.9) but it performs

poorer than EMLE in the presence of exponential, Gamma and Weibull random delays (Figures A.2, A.4-A.6, A.8, and A.10-A.12). This happens because Gamma and Weibull random delays are closer to the exponential random delay.

3.2 Combination of Clock Offset and Skew Estimation Based on GMKPF

In this section, computer simulation results will be presented to determine the performance of GMKPF (Section 2.7), JMLE for Gaussian and exponential delay models (Section 2.4), and MLLE for Gaussian and exponential delay models (Section 2.5) for estimating the clock offset and skew in WSNs. The observation noise delay model is the same as in Section 3.1. The state transition matrix A of process equation is 0.99999. The process noise v_k is assumed to be Gaussian with constant diagonal matrix covariance:

$$\mathrm{Q} = \begin{bmatrix} 1e-5 & 0 \\ 0 & 1e-5 \end{bmatrix}.$$

The number of particles and GMM components are 1000 and 5, respectively. The experiment was done using Matlab and ReBEL Toolkit. Figure 3.2 shows a plot of the clock offset and clock skew estimation for each Monte Carlo simulation. The MSE performances of estimators are averaged over 2,000 Monte Carlo runs.

Figures B.1-B.6 show the MSE of the estimators assuming that the random delays assume symmetric Gaussian, exponential, asymmetric Gaussian, exponential, Gamma, and Weibull distributions, respectively. The number of observations conducted in this simulation are 10, 15, 20, 25 and 30, respectively.

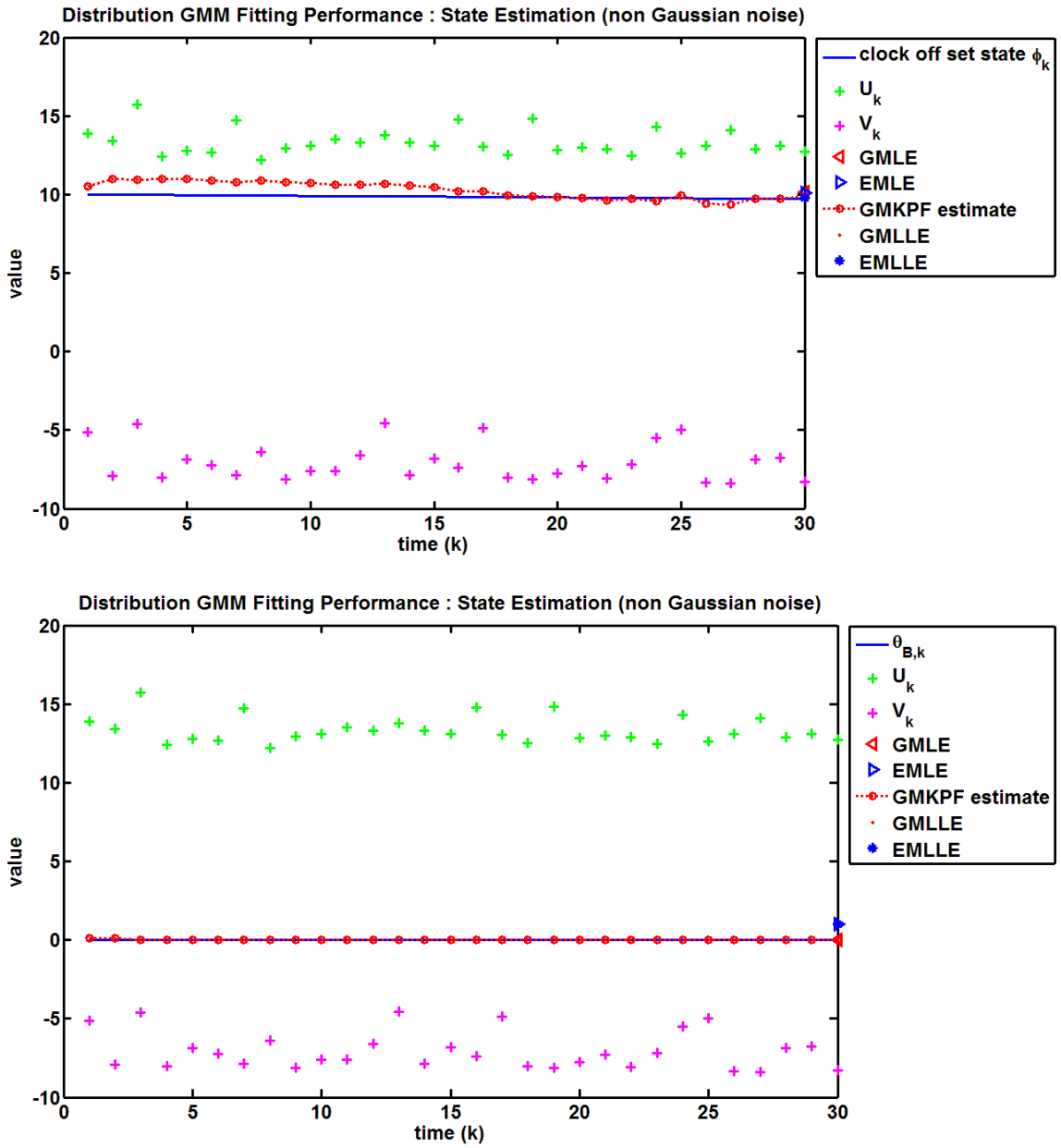

Figure 3.2: Clock offset and skew state estimation via GMKPF.

In the symmetric Gaussian delay case, Figure B.1, GMKPF and GMLE give almost the same performance in estimating the clock skew. However, GMKPF performs

better in estimating the clock offset. Notice that EMLE always give as a value: Not a Number (NaN) for any number of observations. This happens because the possible clock skew parameters (2.11) are not in the valid region (see equations (2.12) and (2.13)). MLLE performs poorer than MLE and GMKPF in estimating jointly the clock offset and skew.

In the symmetric exponential delay case, Figure B.2, GMKPF gives slightly poorer MSE performance in estimating clock skew when compared to EMLE. GMKPF gives better MSE performance in estimating clock offset than EMLE, GMLE, GMLLE, and EMLLE. GMLE performs poorer than GMKPF and EMLE for joint estimation of clock offset and skew estimation. Both GMLLE and EMLLE give relatively the same performance and are poorer than MLE and GMKPF for clock offset and clock skew estimation.

In other cases, Figures B.3-B.6, GMKPF performs better than MLEs and MLLEs in estimating both the clock offset and skew.

Note that EMLE performs better GMLE in the exponential delay case but EMLE is very sensitive to other delay models, especially the Gaussian delay. It is interesting to note that the MSE of GMLE exhibits better performance than MLLE in estimating the clock skew parameter for any delay distributions. GMLE gives poorer performance in estimating the clock offset for Gamma and Weibull delay models which are closer to the exponential distribution than the Gaussian distribution. In addition, EMLLE and GMLLE give almost the same performance in estimating the clock skew parameter regardless of the type of random delays. This is due to the fact that the performance of

the MLLE is dominated by the set of distances $\left(\left\{D_{(i)}\right\}_{i=1}^{4}\right)$, which do not vary much with respect to the type of random delays.

To quantify the robustness of the estimators further, Figures B.7-B.12 show the MSE performance of the GMKPF, GMLE, EMLE, GMLLE, and EMLLE under a mixture of two network delay distributions. The numbers of observations which are experimented are 10, 16, 22, and 28, respectively.

GMKPF clearly outperforms the other estimators in every case. GMLE gives better performance than EMLE, GMLLE and EMLLE if the network delay model is closer to a Gaussian (Figures B.7-B.9). EMLE gives a NaN value in the case that the network delay is a mixture of Gaussian and other delay models (Figures B.7-B.9) and performs better than GMLE and MLLEs in case that the network delay is closer to the exponential delay model (Figures B.10-B.12). GMLLE and EMLLE give almost the same performance for estimating the clock skew parameter. However, when they estimate the clock offset, the MSE performance diverges (Figures B.7-B.11). This shows that MLLEs are not robust to a mixing network delay model.

CHAPTER IV

CONCLUSIONS AND RECOMMENDATIONS

4.1 Conclusions

A joint clock offset and skew estimation method was developed based on GMKPF and its robustness tested via computer simulations. The final results are:

- GMKPF yields the best MSE performance relative to the most commonly proposed estimators in the presence of non-deterministic network delays distributions: Gaussian, exponential, Gamma, and Weibull, and mixture between two of these distributions.
- The main drawback of GMKPF is its computational complexity. In addition, it takes considerable time in terms of calculation. However, GMKPF could yield the same MSE performance as MLE and MLLE in the case of lower number of message exchanges.

4.2 Recommendations

GMKPF's performance depends on the number of particles and the number of Gaussian mixture components. Although, increasing the number of particles and GMM components lead to better performance, it requires a longer time in terms of completing the required computations. GMKPF could be studied further to identify the best number of particles and GMM components in estimating the clock offset and skew. GMKPF's performance is also very sensitive to the process state transition matrix A (2.29), process

noise and initialisation of GMKPF estimator. The performance can vary drastically due to changes in these parameters. Thus, GMKPF could give even better performance, provided there is a study to determine the optimal values of these parameters.

REFERENCES

[1] E. Serpedin and Q. M. Chaudhari, *Synchronization in Wireless Sensor Networks : Parameter Estimation, Performance Benchmarks and Protocols*. New York: Cambridge University Press, 2009.

[2] I. F. Akyildiz, W. Su, Y. Sankarasubramaniam, and E. Cayirci, "Wireless sensor networks: a survey," *Computer Networks*, vol. 38, no. 4, pp. 393-422, Mar 15, 2002.

[3] H. S. Abdel-Ghaffar, "Analysis of synchronization algorithms with time-out control over networks with exponentially symmetric delays,", *IEEE Trans. on Communications*, vol. 50, no. 10, pp. 1652-1661, 2002.

[4] J. Kim, J. Lee, E. Serpedin, and K. Qaraqe, "A robust estimation scheme for clock phase offsets in wireless sensor networks in the presence of non-Gaussian random delays," *Signal Processing*, vol. 89, no. 6, pp. 1155-1161, 2009.

[5] A. Leon-Garcia, *Probability and Random Processes for Electrical Engineering*, 2nd ed. Reading, MA: Addison-Wesley, 1994.

[6] A. Papoulis, *Probability, Random Variables, and Stochastic Processes*. New York: McGraw-Hill, 2002.

[7] J. Elson, L. Girod, and D. Estrin, "Fine-grained network time synchronization using reference broadcasts," in *Proc. of the Fifth Symposium on Operating System Design and Implementation*, Boston, MA, Dec. 2002.

[8] K.-L. Noh, Q. M. Chaudhari, E. Serpedin, and B. W. Suter, "Novel clock phase offset and skew estimation using two-way timing message exchanges for wireless sensor networks," *IEEE Trans. on Communications,* vol. 55, no. 4, pp. 766-777, April 2007.

[9] S. Ganeriwal, R. Kumar and M. B. Srivastava, "Timing-sync protocol for sensor networks," in *Proc. First Int. Conf. Embedded Network Sensor Systems*, pp. 138-149, 2003.

[10] D. R. Jeske, "On maximum-likelihood estimation of clock offset," *IEEE Trans.s on Communications,* vol. 53, no. 1, pp. 53-54, 2005.

[11] Q. M. Chaudhari, E. Serpedin, and K. Qaraqe, "On maximum likelihood estimation of clock offset and skew in networks with exponential delays," *IEEE Trans. on Signal Processing,* vol. 56, no. 4, pp. 1685-1697, 2008.

[12] P. M. Djuric, J. H. Kotecha, J. Zhang, Y. Huang, and T. Ghirmai, "Particle filtering," *IEEE Signal Processing Magazine,* vol. 20, pp. 19-38, 2003.

[13] R. van der Merwe and E. Wan, "Gaussian mixture sigma-point particle filters for sequential probabilistic inference in dynamic state-space models," in *Proc. IEEE Int. Conf. Acoustics, Speech, and Signal Processing,* vol. 6, pp. VI-701-4, 2003.

[14] R. van der Merwe and E. Wan, "Sigma-point kalman filters for probabilistic inference in dynamic state-space models," in *Proc. Workshop Advances in Machine Learning,* Montreal, Canada, Jun 2003.

[15] D. Alspach and H. Sorenson, "Nonlinear Bayesian estimation using Gaussian sum approximations," *IEEE Trans. on Automatic Control* vol. 17, pp. 439-448, 1972.

[16] S. M. Kay, *Fundamentals of Statistical Signal Processing*. Englewood Cliffs, NJ: PTR Prentice-Hall, 1993.

[17] A. Doucet, N. de Freitas, and N. Gordon, *Sequential Monte Carlo Methods in Practice*. New York: Springer, 2001.

[18] G. J. McLachlan and T. Krishnan, *The EM Algorithm and Extensions*, 2nd ed. Hoboken, NJ: Wiley Interscience, 2008.

APPENDIX A

MSE PERFORMANCE OF CLOCK OFFSET ESTIMATION BASED ON GMKPF

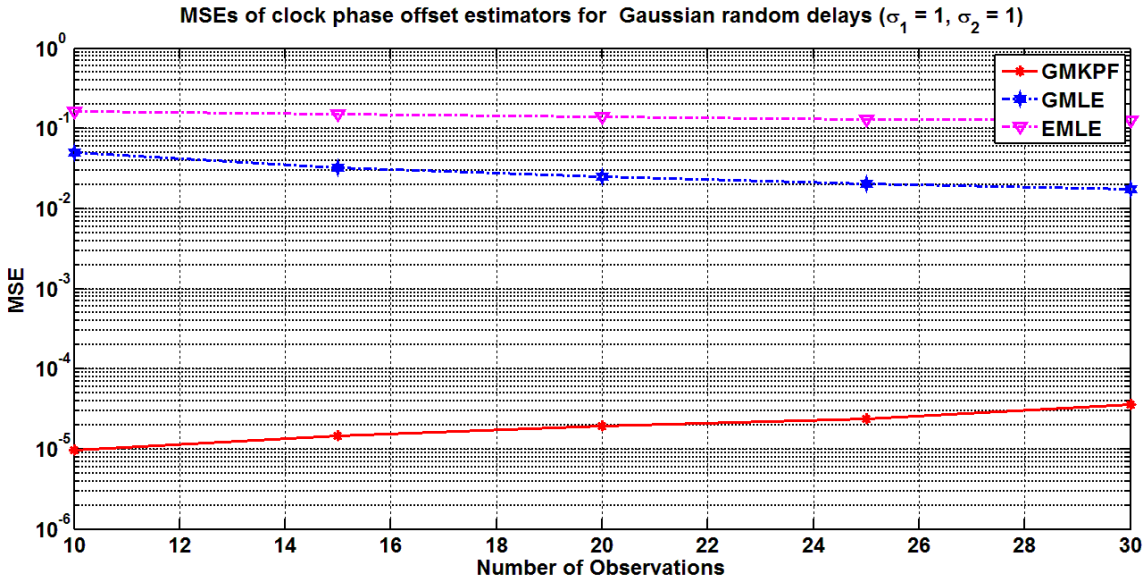

Figure A.1: MSEs of clock offset estimators for symmetric Gaussian delays [σ =1].

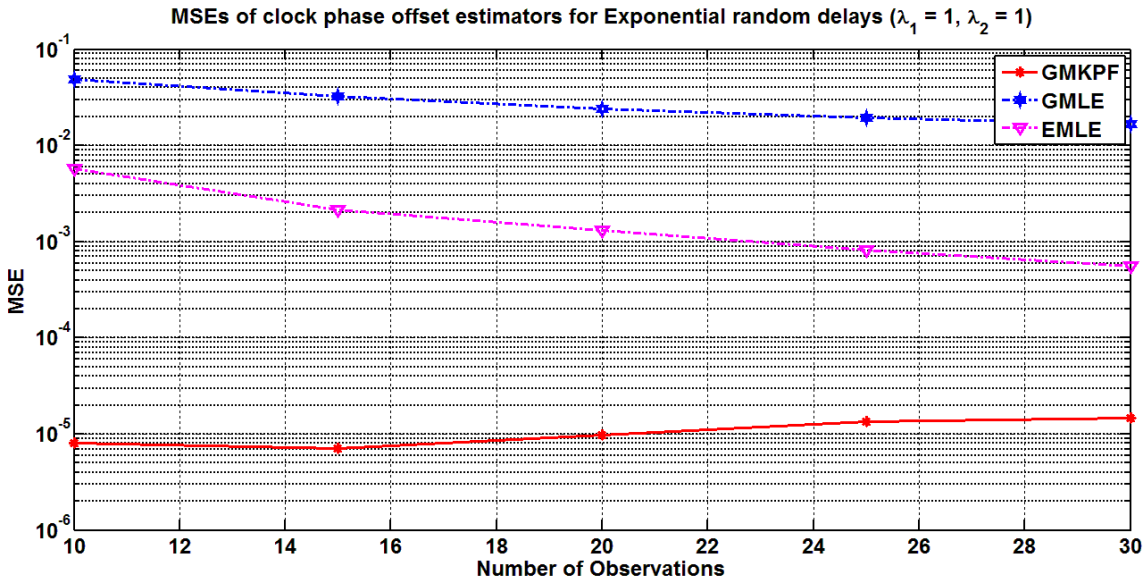

Figure A.2: MSEs of clock offset estimators for symmetric exponential random delays [λ=1].

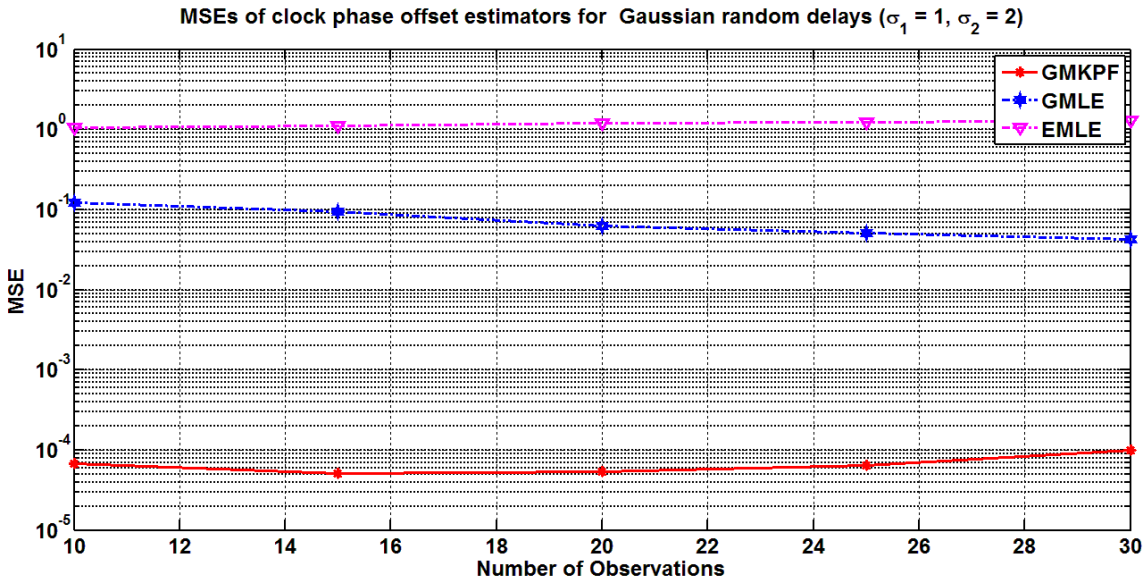

Figure A.3: MSEs of clock offset estimators for asymmetric Gaussian random delays [σ_1=1, σ_2=2].

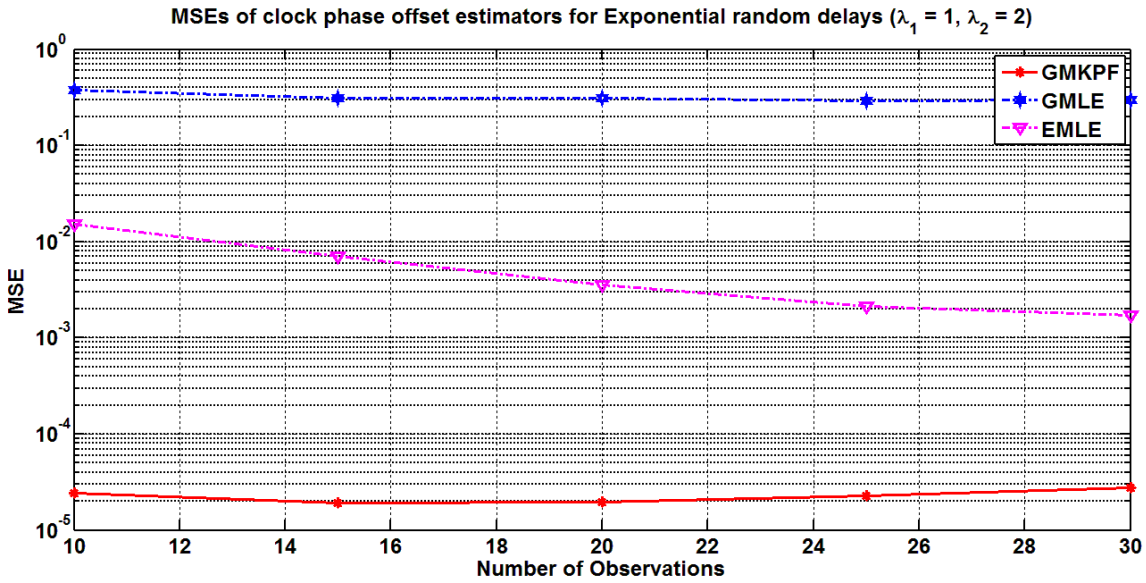

Figure A.4: MSEs of clock offset estimators for asymmetric exponential random delays [λ_1=1, λ_2=2].

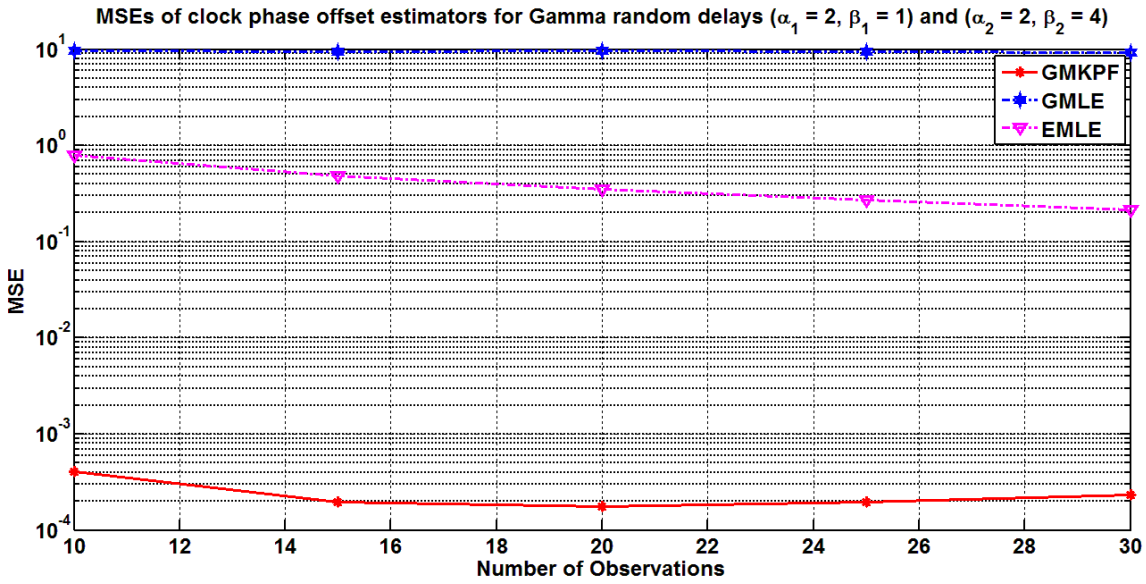

Figure A.5: MSEs of clock offset estimators for Gamma random delays [(α_1=2, β_1=1) and (α_2=2, β_2=4)].

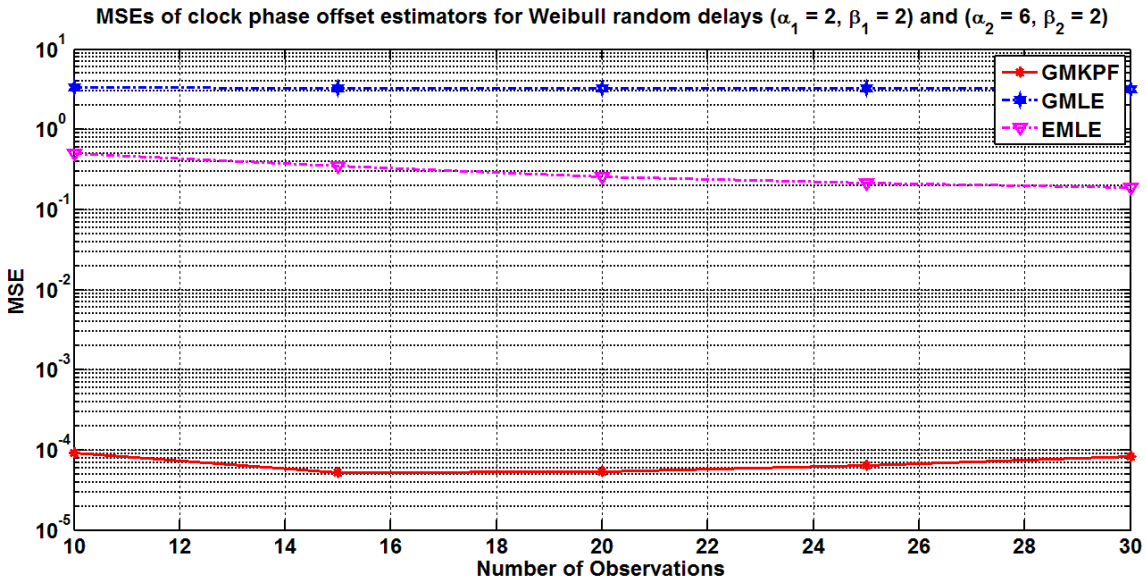

Figure A.6: MSEs of clock offset estimators for Weibull random delays [(α_1 =2, β_1=2) and (α_2 =6, β_2 =2)].

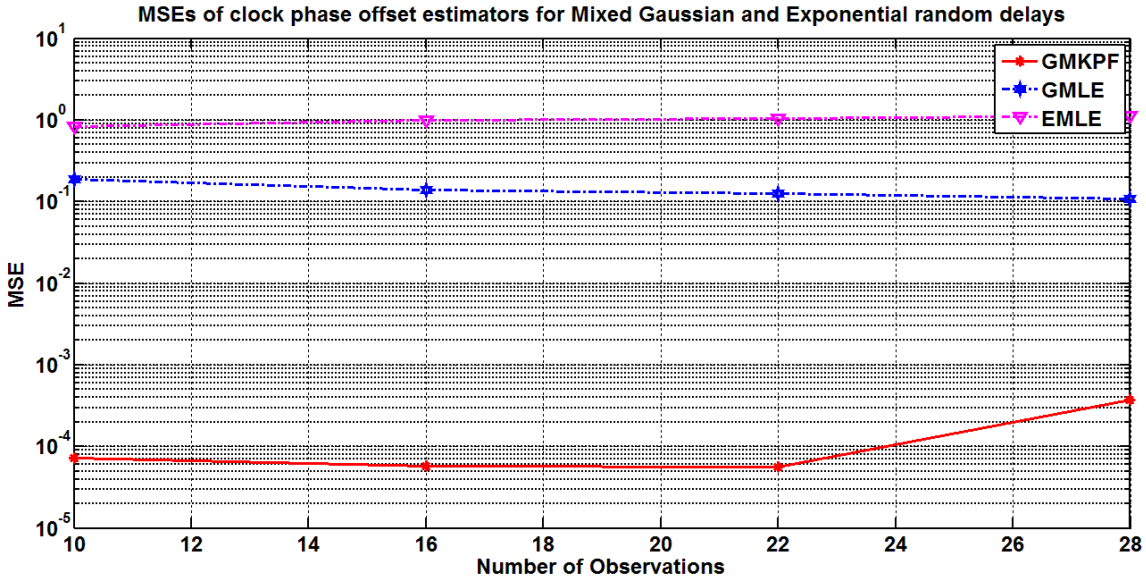

Figure A.7: MSEs of clock offset estimators for a mixture of Gaussian [σ_1 =1, σ_2 =2] and exponential [λ_1 =1, λ_2 =2] random delays.

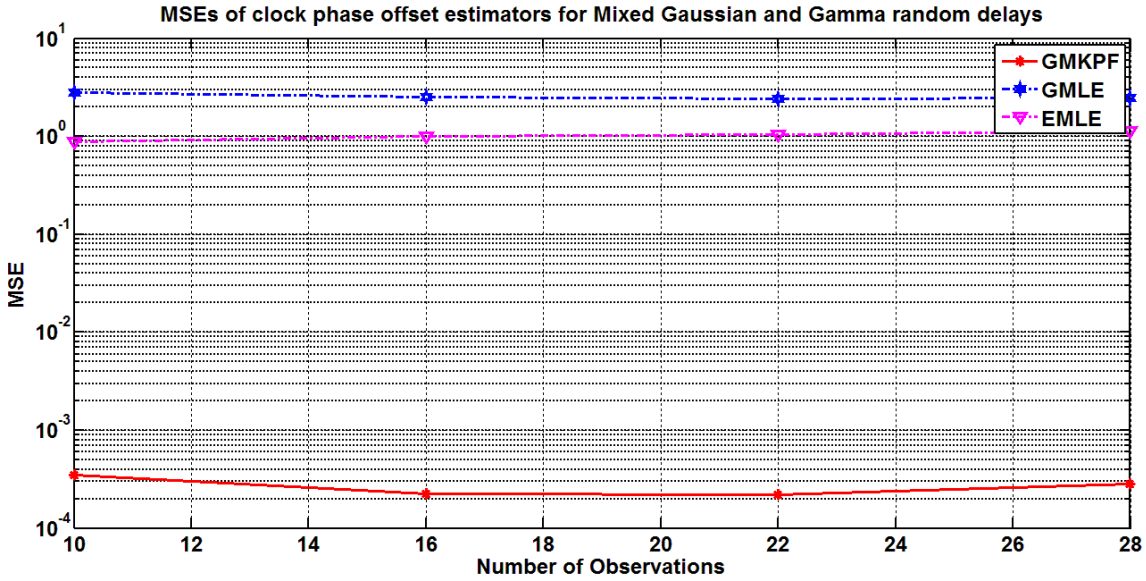

Figure A.8: MSEs of clock offset estimators for a mixture of Gaussian $[\sigma_1=1,\ \sigma_2=2]$ and Gamma $[(\alpha_1=2,\ \beta_1=1)$ and $(\alpha_2=2,\ \beta_2=4)]$ random delays.

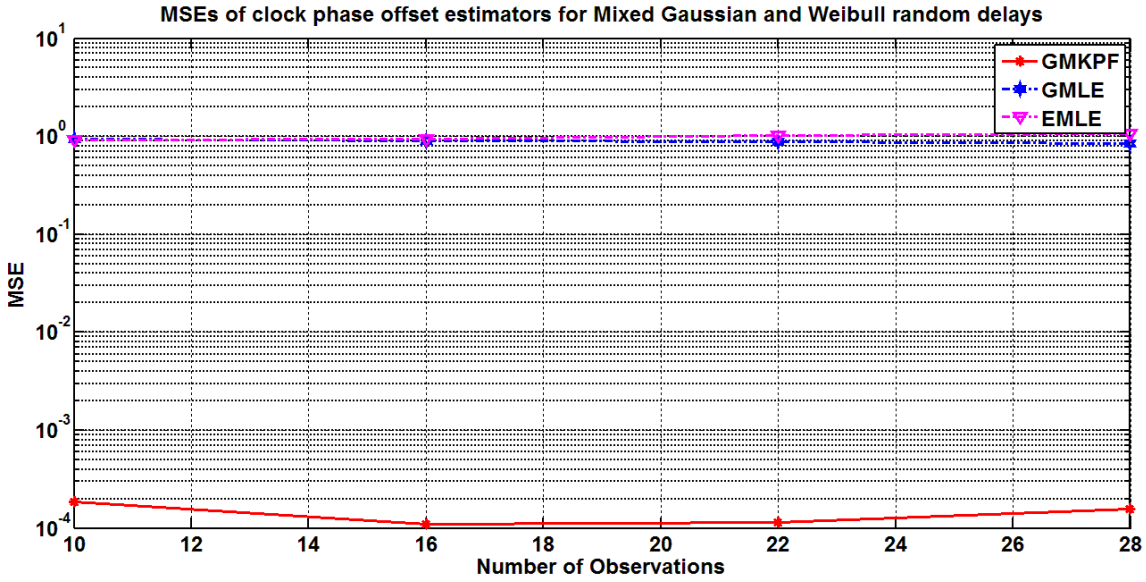

Figure A.9: MSEs of clock offset estimators for a mixture of Gaussian $[\sigma_1=1,\ \sigma_2=2]$ and Weibull $[(\alpha_1=2,\ \beta_1=2)$ and $(\alpha_2=6,\ \beta_2=2)]$ random delays.

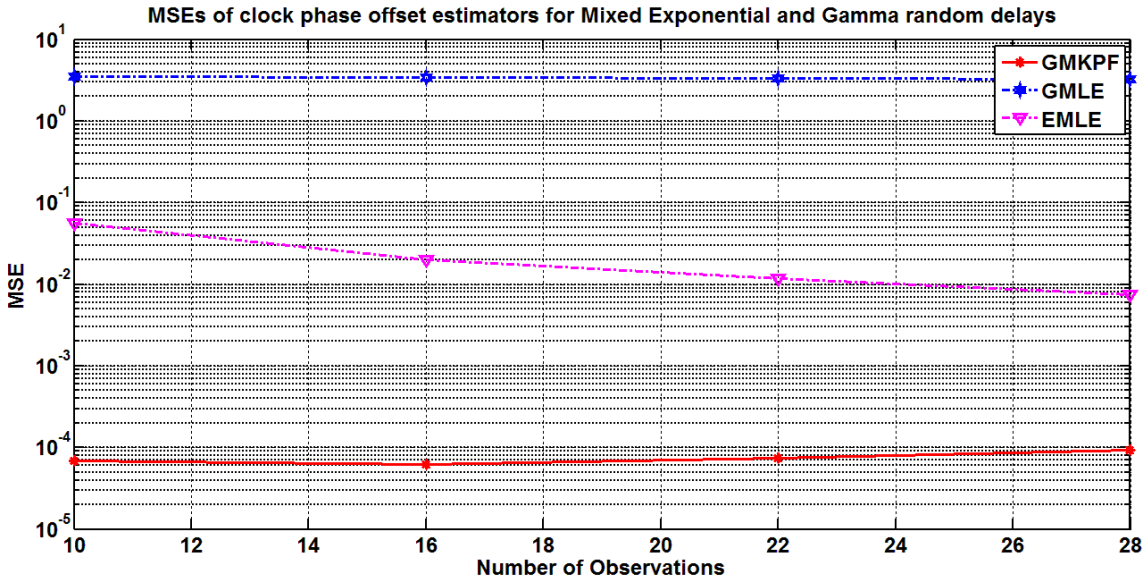

Figure A.10: MSEs of clock offset estimators for a mixture of exponential [λ_1=1, λ_2=2] and Gamma [(α_1=2, β_1=1) and (α_2=2, β_2=4)] random delays.

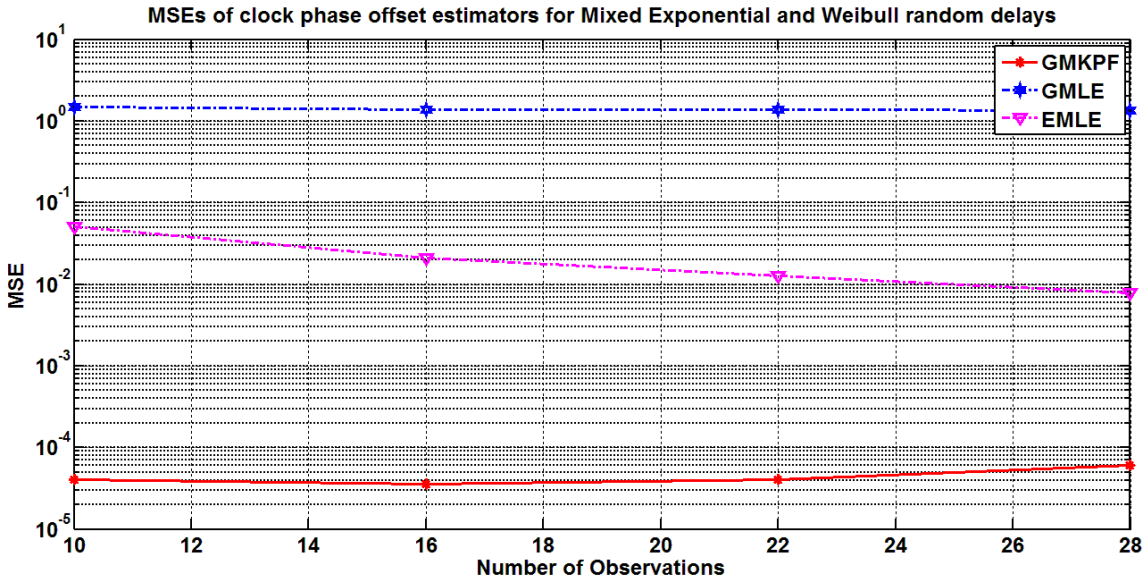

Figure A.11: MSEs of clock offset estimators for a mixture of exponential [λ_1=1, λ_2=2] and Weibull [(α_1=2, β_1=2) and (α_2=6, β_2=2)] random delays.

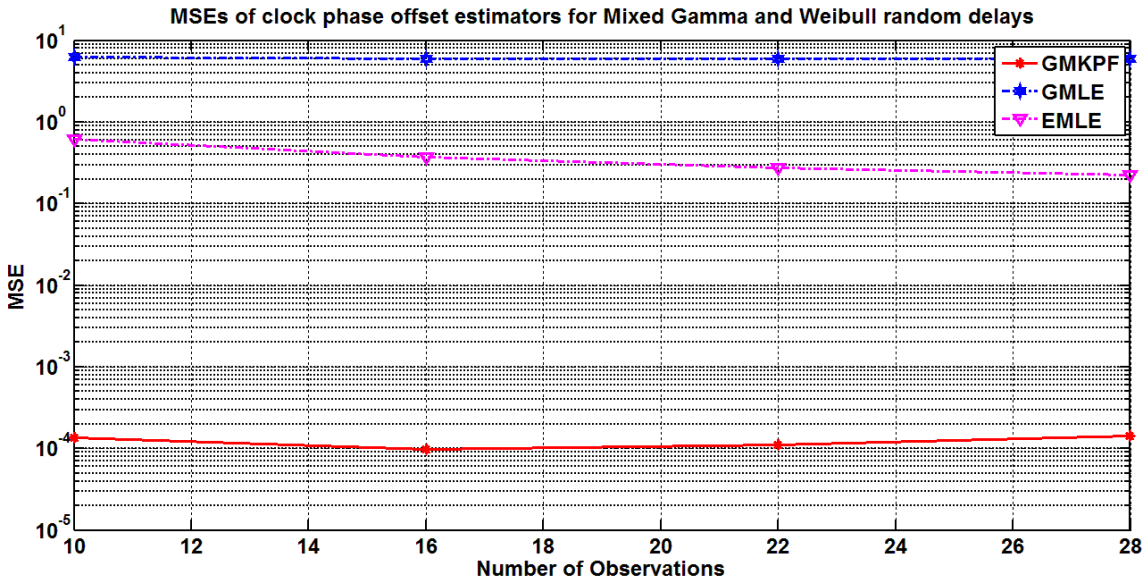

Figure A.12: MSEs of clock offset estimators for a mixture of Gamma [(α_1 =2, β_1=1) and (α_2 =2, β_2 =4)] and Weibull [(α_1 =2, β_1=2) and (α_2 =6, β_2 =2)] random delays.

APPENDIX B

MSE PERFORMANCE OF CLOCK OFFSET AND SKEW ESTIMATION BASED ON GMKPF

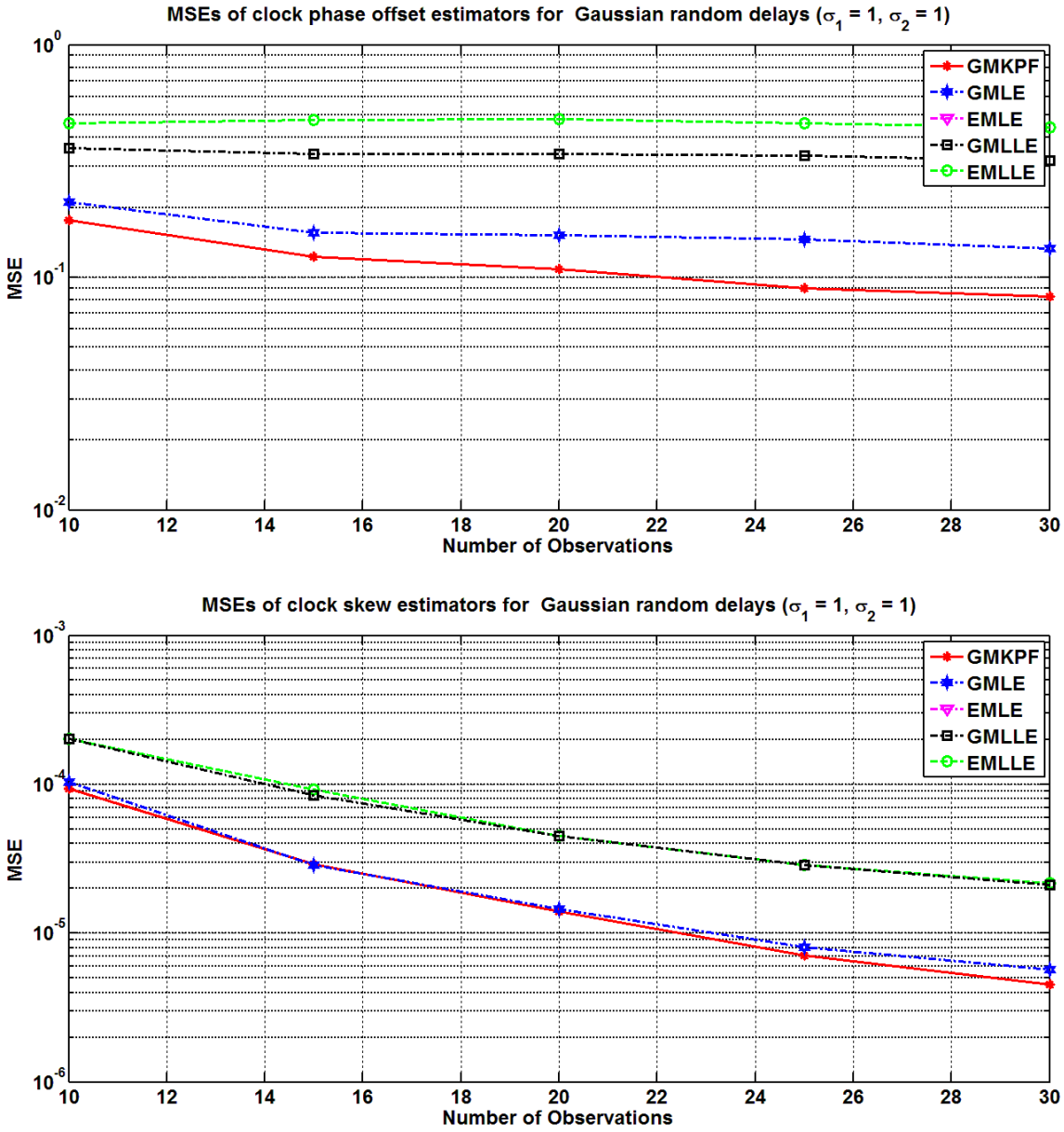

Figure B.1: MSEs of clock offset and skew estimators for symmetric Gaussian random delays [σ =1].

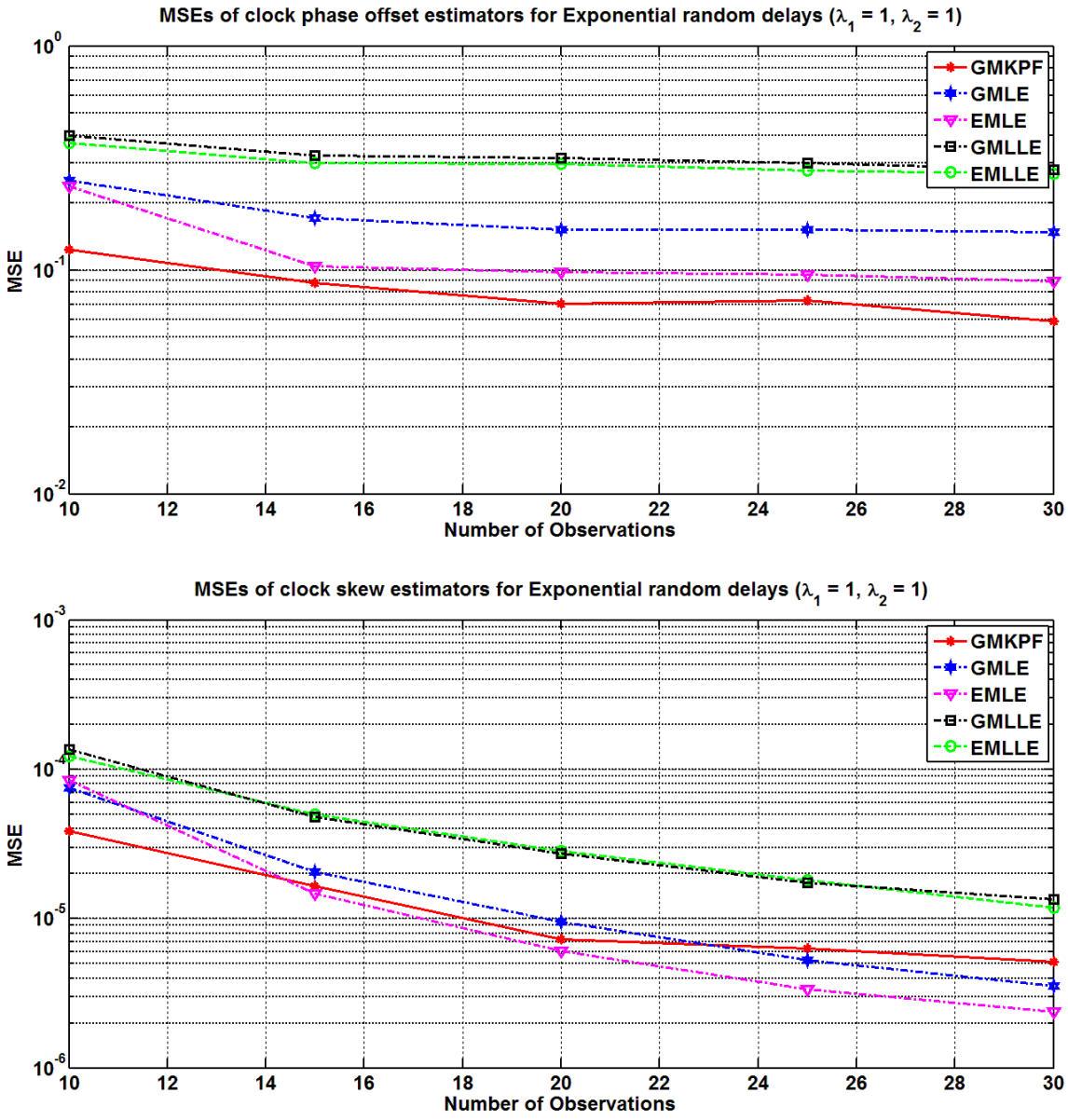

Figure B.2: MSEs of clock offset and skew estimators for symmetric exponential random delays [λ =1].

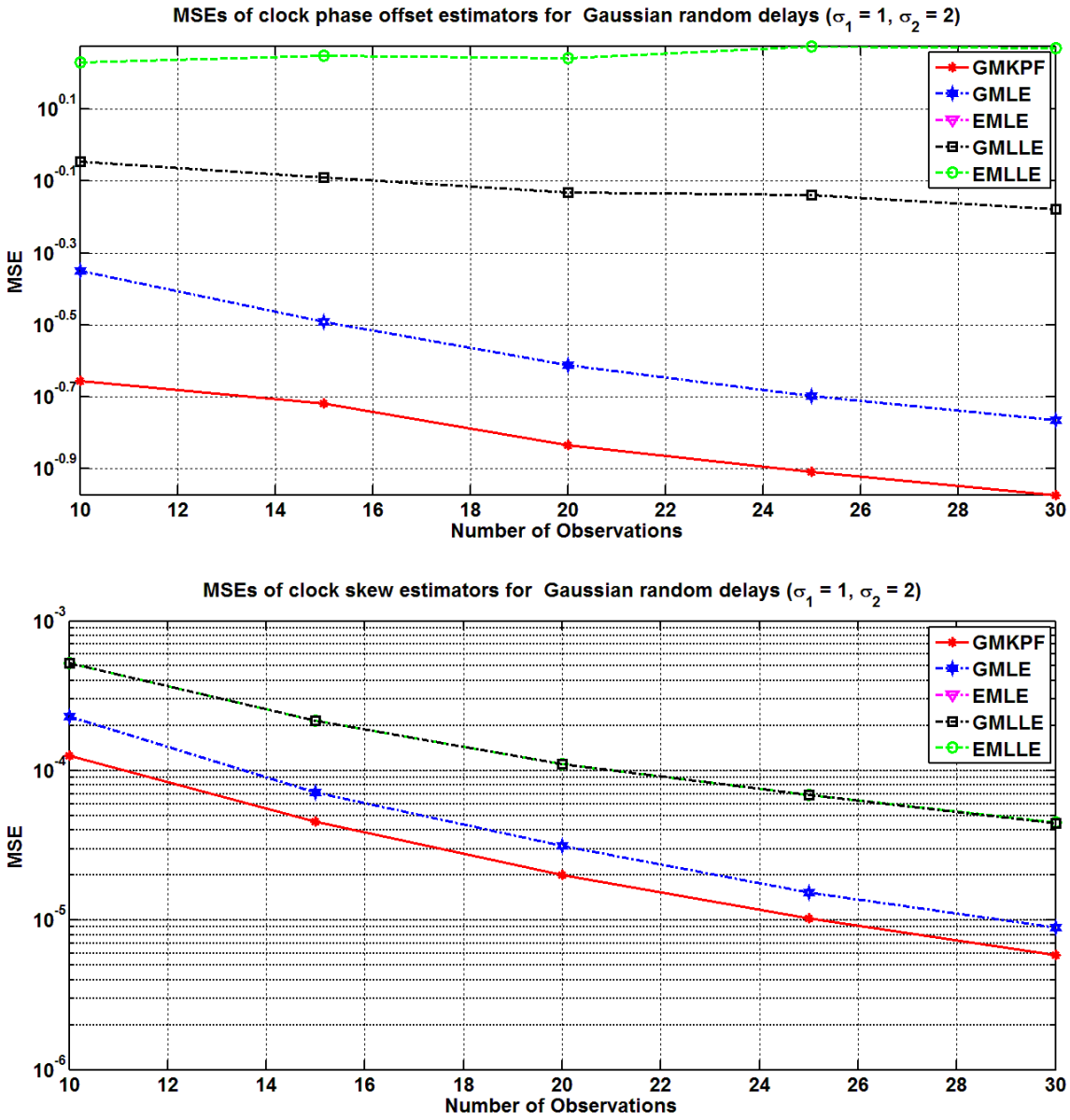

Figure B.3: MSEs of clock offset and skew estimators for asymmetric Gaussian random delays [σ_1=1, σ_2=2].

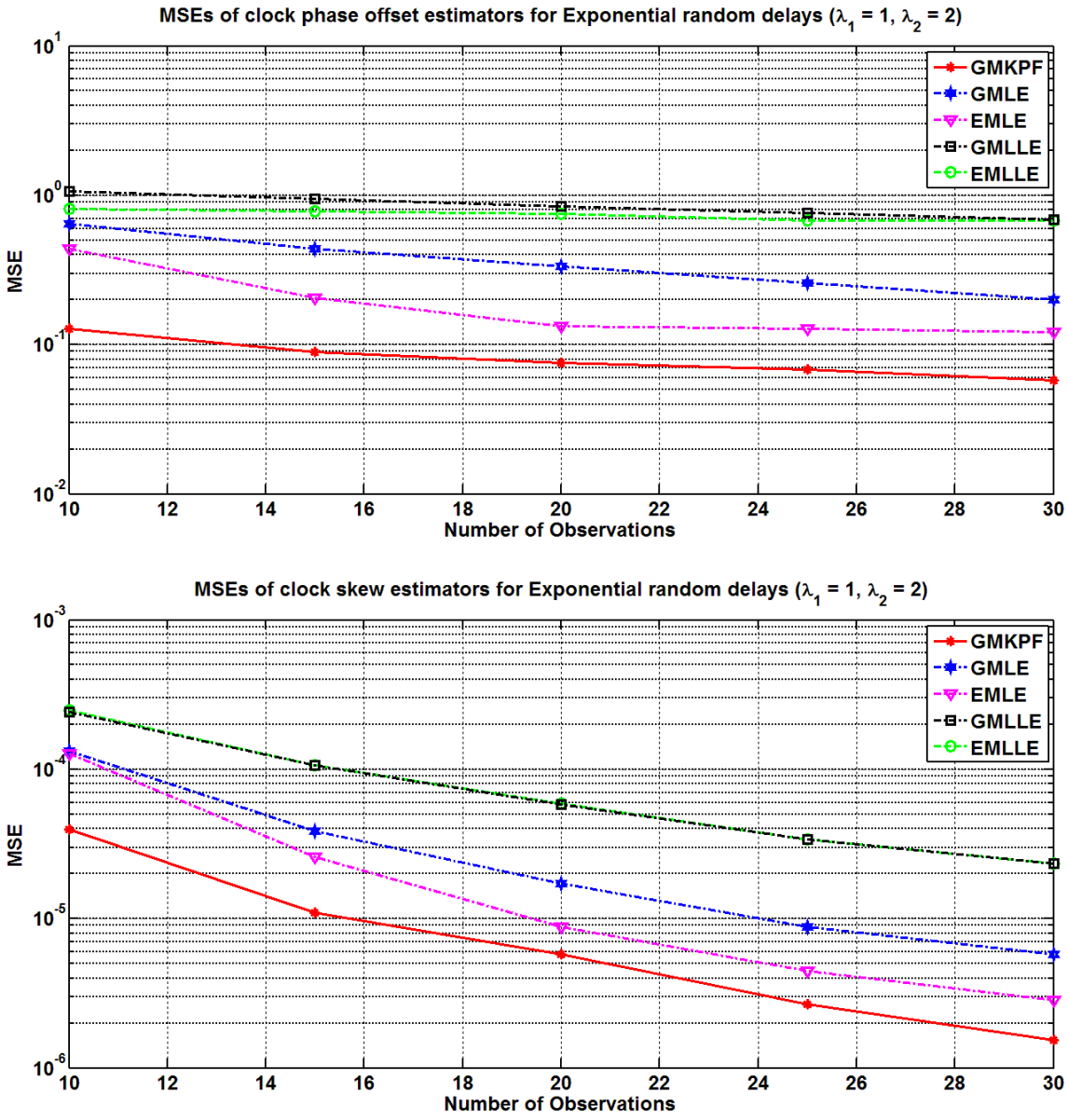

Figure B.4: MSEs of clock offset and skew estimators for asymmetric exponential random delays [λ_1=1, λ_2 =2].

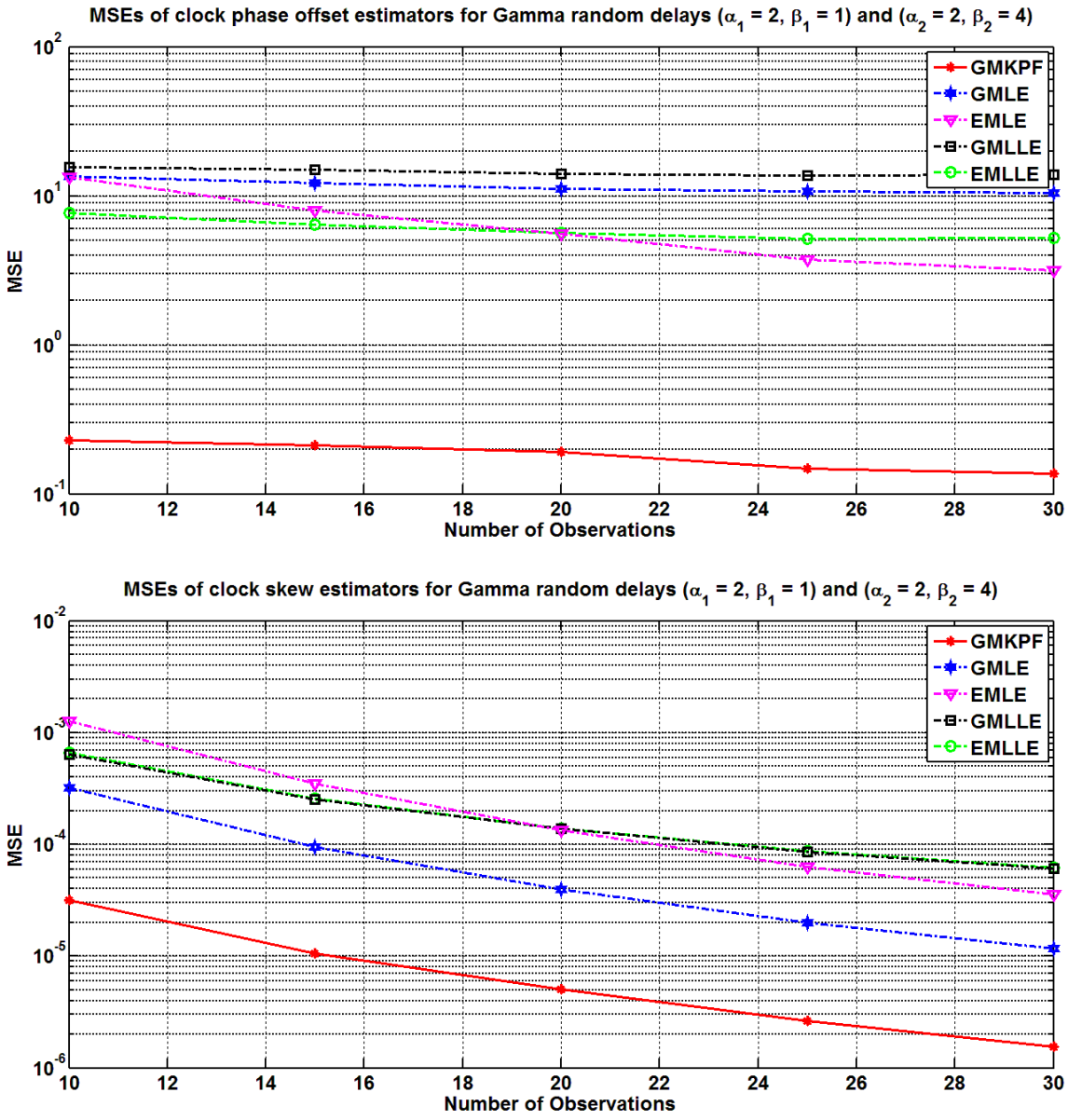

Figure B.5: MSEs of clock offset and skew estimators for Gamma random delays [(α_1=2, β_1=1) and (α_2=2, β_2=4)].

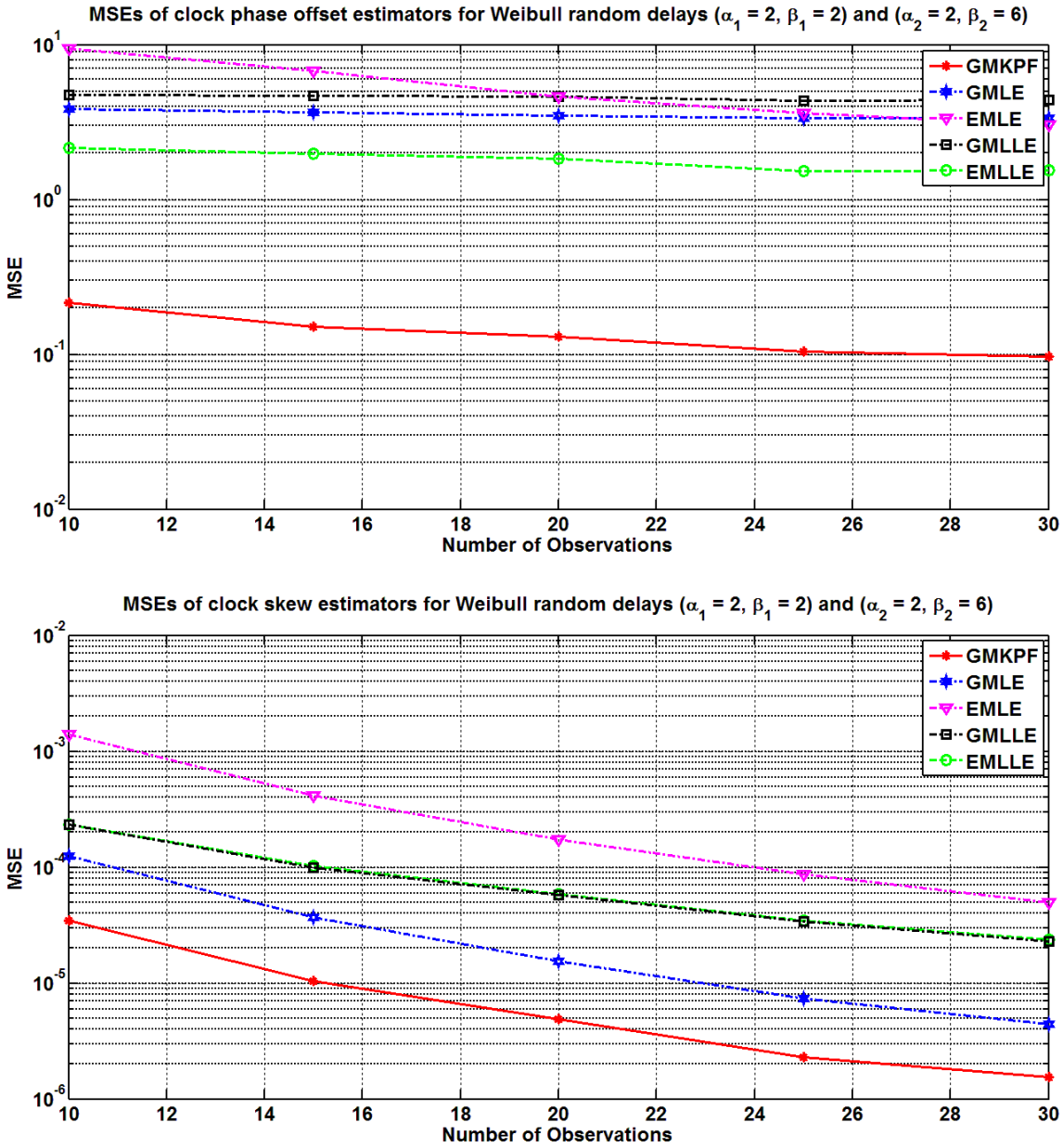

Figure B.6: MSEs of clock offset and skew estimators for Weibull random delays [(α_1=2, β_1=2) and (α_2=6, β_2=2)].

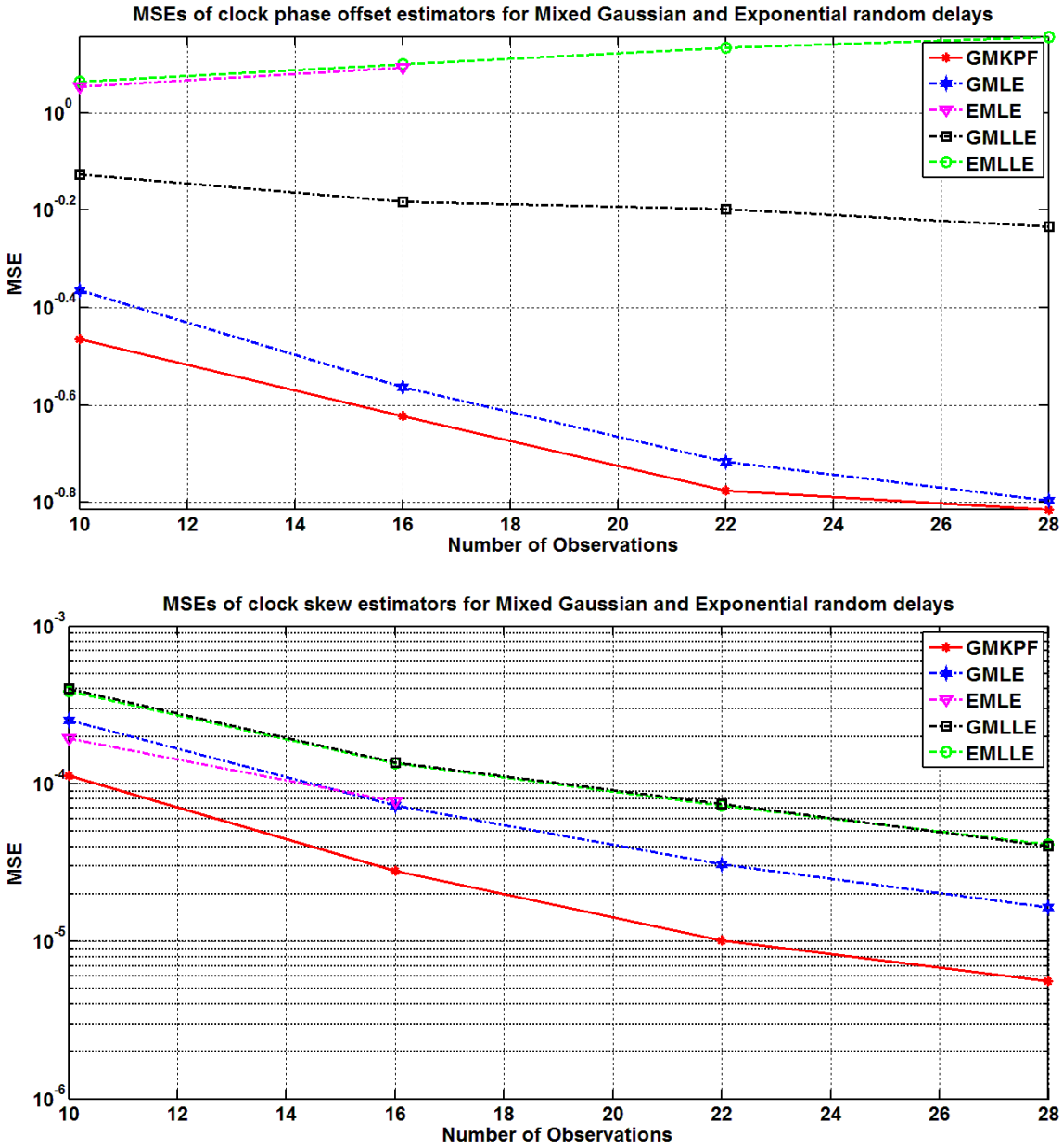

Figure B.7: MSEs of clock offset and skew estimators for a mixture of Gaussian [σ_1=1, σ_2=2] and exponential [λ_1=1, λ_2=2] random delays.

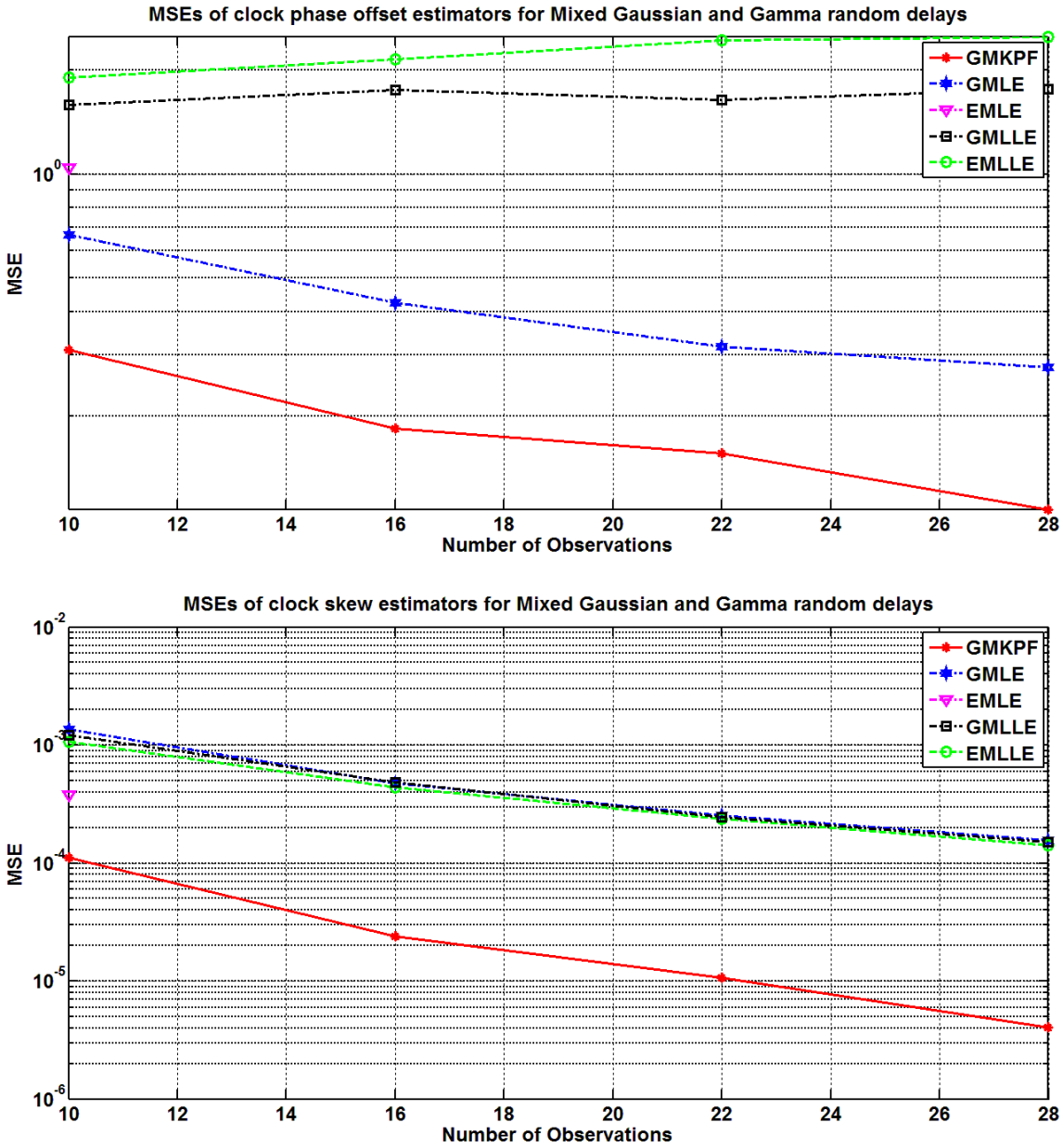

Figure B.8: MSEs of clock offset and skew estimators for a mixture of Gaussian [σ_1=1, σ_2=2] and Gamma [(α_1=2, β_1=1) and (α_2=2, β_2=4)] random delays.

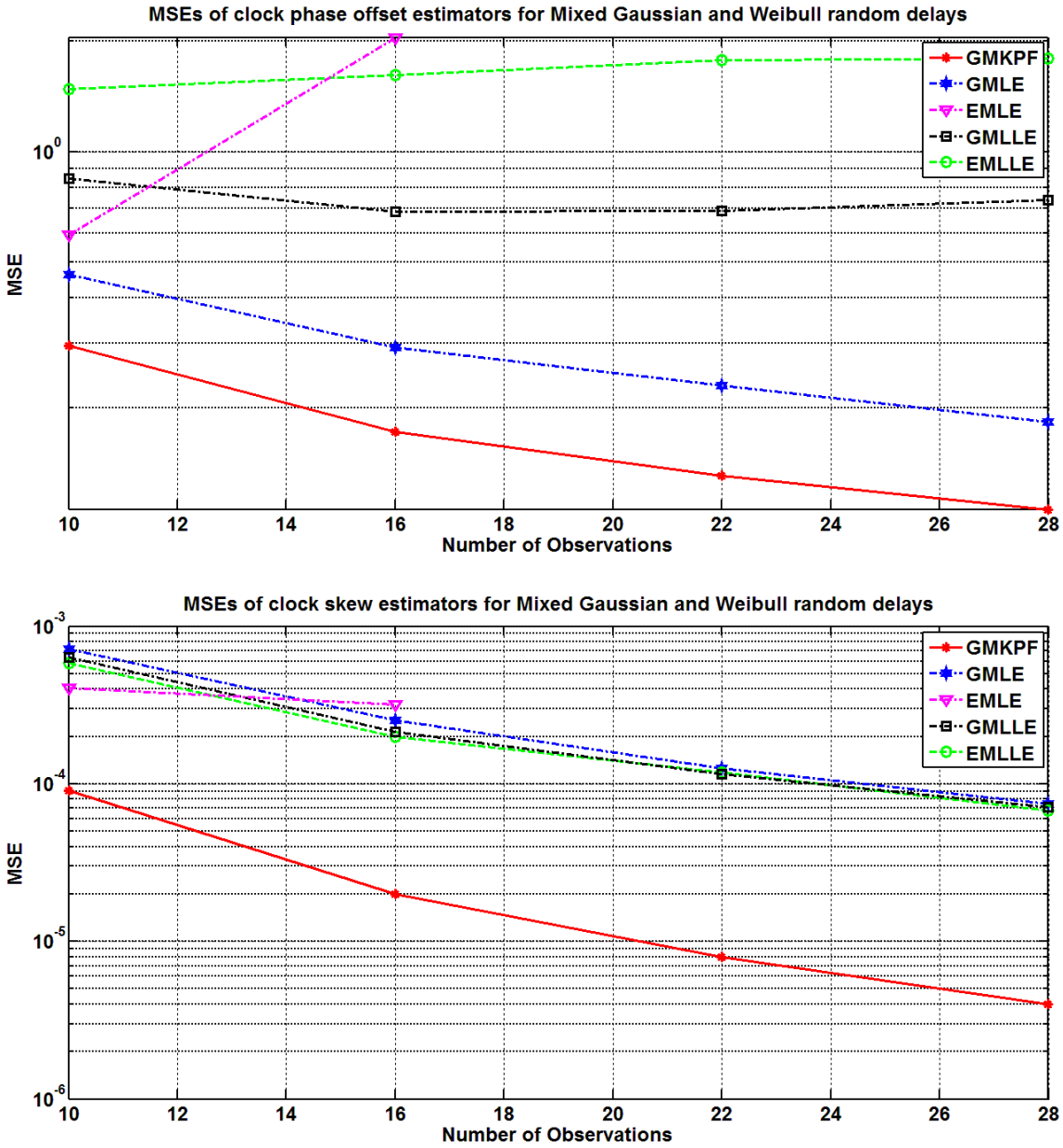

Figure B.9: MSEs of clock offset and skew estimators for a mixture of Gaussian [σ_1=1, σ_2=2] and Weibull [(α_1=2, β_1=2) and (α_2=6, β_2=2)] random delays.

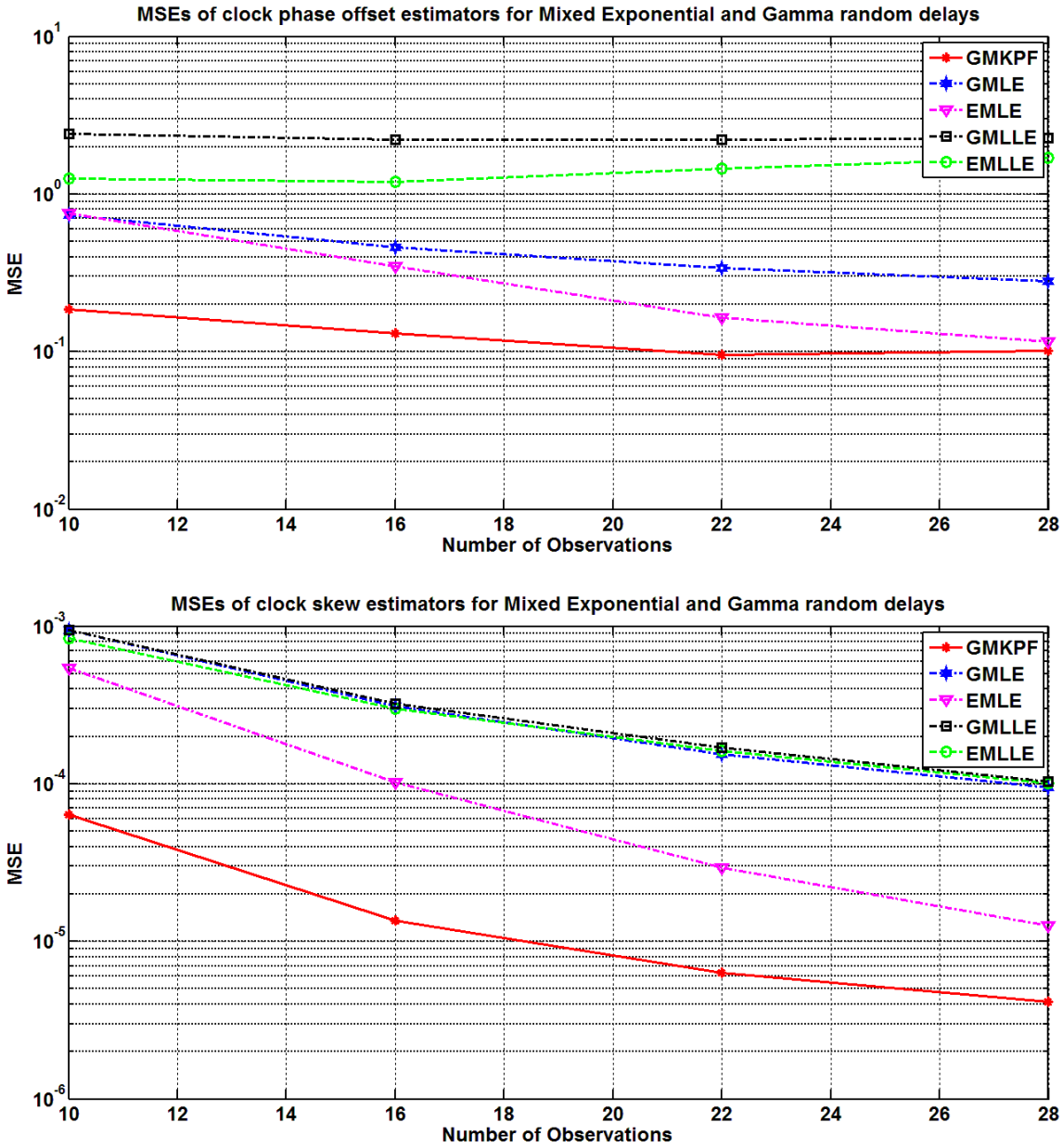

Figure B.10: MSEs of clock offset and skew estimators for a mixture of exponential [λ_1=1, λ_2=2] and Gamma [(α_1=2, β_1=1) and (α_2=2, β_2=4)] random delays.

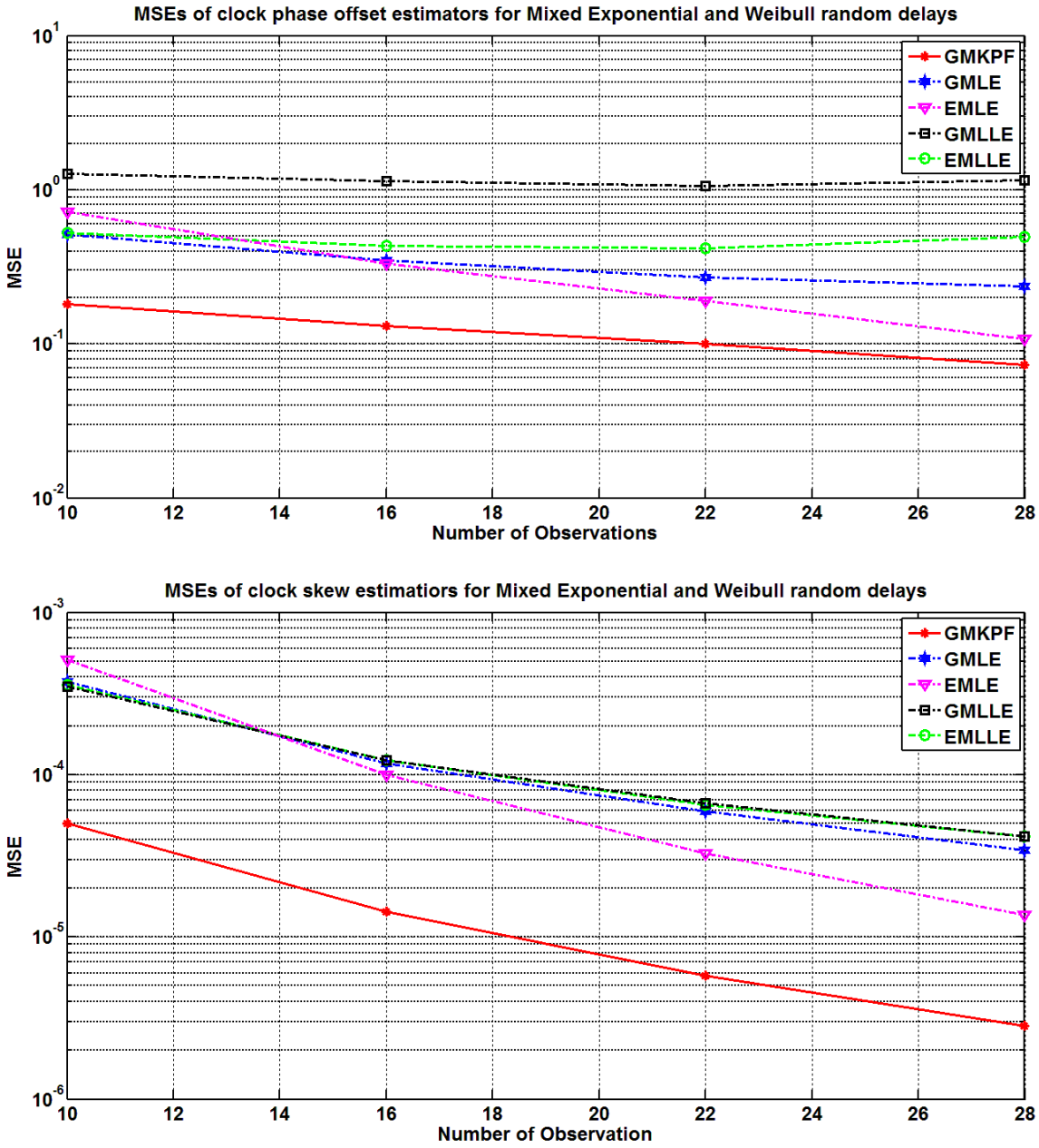

Figure B.11: MSEs of clock offset and skew estimators for a mixture of exponential [λ_1=1, λ_2=2] and Weibull [(α_1=2, β_1=2) and (α_2=6, β_2=2)] random delays.

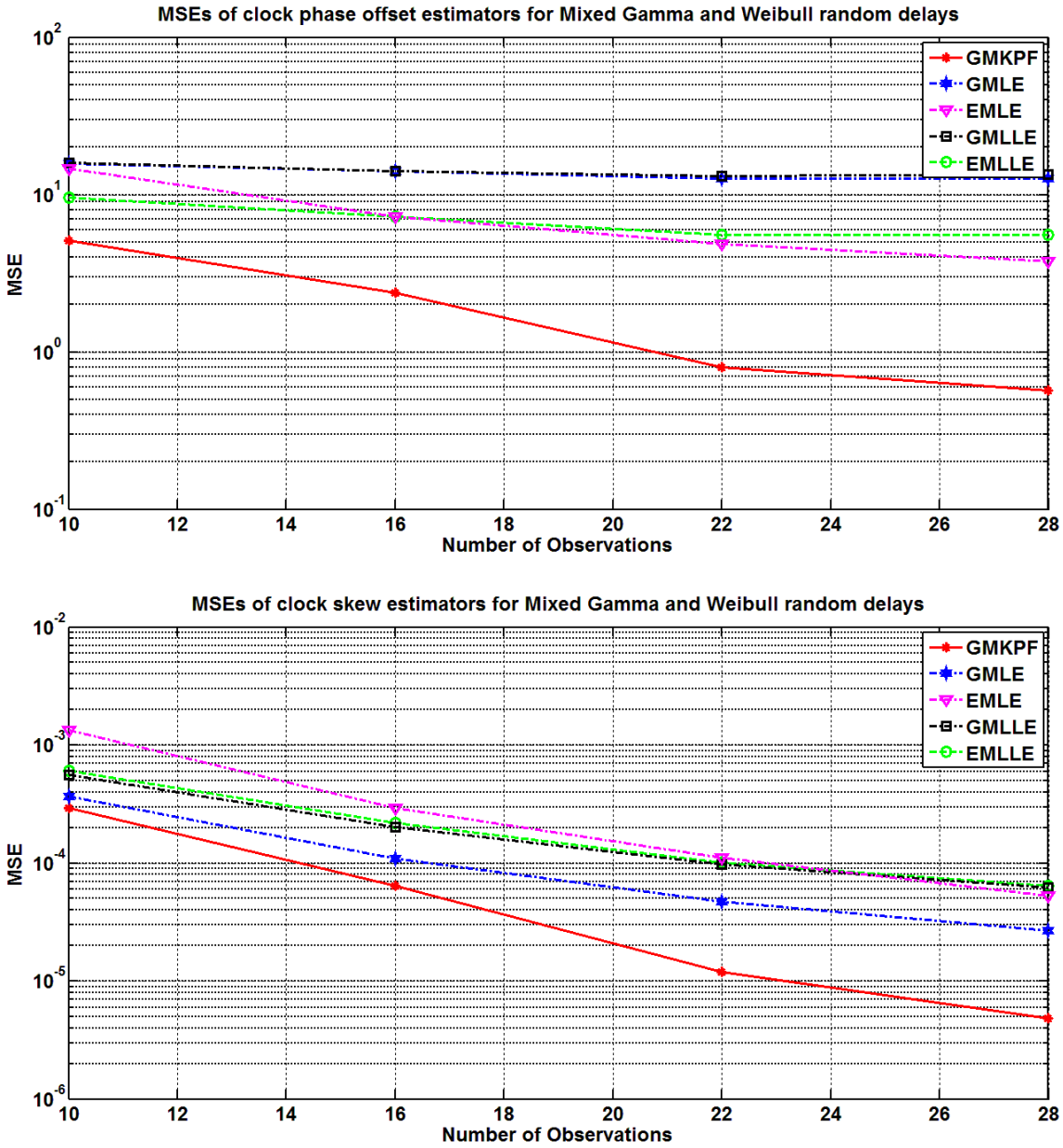

Figure B.12: MSEs of clock offset and skew estimators for a mixture of Gamma [(α_1 =2, β_1 =1) and (α_2 =2, β_2 =4)] and Weibull [(α_1 =2, β_1 =2) and (α_2 =6, β_2 =2)] random delays.

VITA

Name: Sawin Saibua

Address: Department of Electrical and Computer Engineering,
Texas A&M University,
214 Zachry Engineering Center,
TAMU 3128 College Station, Texas 77843-3128.

Education: B.Eng., Electrical Engineering,
Chulalongkorn University, Bangkok, Thailand, 2008.

M.S., Electrical Engineering,
Texas A&M University, College Station, 2010.